ANNALS OF GEOPHYSICS, 69, 2026; doi:10.4401/ag-9547
OPEN ACCESS

Lahars at Stromboli volcano (Italy): insights from field and sedimentological data

Roberto Gianardi[*,1,2], Daniele Andronico[3], Marco Pistolesi[1], Claudia Spinetti [4], Marina Bisson[2]

(1) University of Pisa, Earth Sciences Department, Pisa, Italy
(2) Istituto Nazionale di Geofisica e Vulcanologia, Sezione di Pisa, Pisa, Italy
(3) Istituto Nazionale di Geofisica e Vulcanologia, Osservatorio Etneo, Catania, Italy
(4) Istituto Nazionale di Geofisica e Vulcanologia, Osservatorio Nazionale Terremoti, Roma, Italy

Article history: received February 16, 2026; accepted March 23, 2026

Abstract

Stromboli, one of the most active volcanoes in Italy, is characterized by an ordinary eruptive activity consisting of persistent and mild explosions, occasionally interrupted by lava flows and by significant eruptions named major explosions and paroxysms. During such explosive activity, abundant loose pyroclastic material is emplaced on the upper steep slopes of the volcano. Due to intense or prolonged rainfall, this material can be remobilized, thereby generating volcanoclastic flows of different typologies that invade the lower slopes and, in several cases, reach the inhabited coastal areas causing huge damage to infrastructures. The most recent flows occurred on October 18-20, 2024 and May 15, 2025, when Stromboli island was hit by very intense rainfall concentrated in a few tens of minutes. Consequently, loose tephra deposits were rapidly remobilized, triggering lahars that reached the villages of Stromboli and Ginostra, as well as the access routes to the volcano summit. In this work, for the first time, the grain-size characterization of these lahar deposits is presented. Based on the sedimentological characteristics and grain-size distributions the deposits have been classified as hyperconcentrated stream flows and proves to be dominated by coarse to fine ash. Moreover, using high-resolution Pleiades optical satellite data, one of the depositional fans sampled during fieldwork was characterized. The results of this study provide the first quantitative grain-size dataset for Stromboli lahars, representing a key constraint for the reconstruction and numerical modeling of these processes in volcanic hazard assessment at Stromboli.

Keywords: Stromboli; Lahar deposit; Grain-size analysis; Hyperconcentrated flows; Satellite data

1. Introduction

Lahars, defined as gravity-driven, water-saturated flows composed of volcanic debris (Vallance and Iverson, 2015), are among the most destructive volcanic hazards worldwide (Witham, 2005). They can be triggered by a variety of mechanisms, including intense or prolonged rainfall, rapid snow or ice melt, crater lake overflows, and volcanic edifice or flank collapse (Pierson et al., 1990; Vallance and Iverson, 2015; Vallance 2024). Lahars formation

requires the coexistence of an adequate water source, an abundant supply of unconsolidated sediment, steep slopes and an effective triggering mechanism (Vallance and Iverson, 2015). At Stromboli volcano, one of the 7 islands of the Aeolian archipelago (Southern Italy), lahars have become an increasingly recurrent phenomenon since August 12, 2022. Most of the supply sediment that triggered lahars was generated during the 2019 eruptive crisis (e.g. Andronico et al., 2021; Giordano and De Astis, 2021) which consisted of 2 paroxysms that produced abundant pyroclastics dispersed over the upper volcanic slopes. In addition, the wildfires occurring in 2019 and 2022 (Ferrentino et al., 2025; Guardo et al., 2024, Iacono et al., 2025) destroyed most of the vegetation/original plants of Mediterranean nature covering the island, characterized by the presence of shrubs in various forms and herbaceous vegetation (Guarino et al., 2024; Iacono et al., 2025), increasing the availability of unconsolidated sediment and reducing slope protection.

Together, these conditions satisfied two of the fundamental prerequisites for lahars generation, that is the abundant sediment supply and steep, unstable slopes. This context was further worsened by the eruptive crisis of 2024, during which a significant volume of volcanic material along the Sciara del Fuoco was remobilized through major landslide events, generating a thick deposit on the upper slope of the volcano and forming a compact, low-permeability layer and further increasing lahar susceptibility. Considering that, particularly during the winter, the island undergoes intense rainfall confined to a few hours/days, all the conditions for lahars generation are met, making these flows one of the most important secondary volcanic hazards at Stromboli.

The combined effect of thick, unconsolidated tephra deposits, the loss of vegetative cover and the presence of an impermeable surface, drastically reduced slope stability and enhanced surface runoff. As a result, in recent years intense rainfall events have rapidly triggered the remobilization of loose pyroclastic material, generating channelized flows that travelled downslope and often reached the coastal areas. The geomorphological setting of Stromboli, with steep flanks and deeply incised gullies, further promotes the mobility and runout of these lahars, which have repeatedly impacted both natural and inhabited sectors of the island.

The main recent events have occurred on August 12, 2022, October 18-20, 2024 and May 15, 2025. In all these cases, highly intense rainfalls caused the formation of multiple lahars that inundated several sectors of the island at different elevations. As summarized in Table 1, these events were characterized by short-duration, high-intensity rainfall, with peak phases lasting less than 3 hours and cumulative precipitation reaching 59.7 mm for the August 12, 2022 event, 14 mm for October 19, 2024, and 29.5 mm for May 15, 2025. In particular, the flows propagated along the main channels, invaded the settlements of Stromboli and Ginostra, and also affected the main routes to the summit. Lahars transported coarse debris, including decimetric to metric-sized blocks, posing severe risks to the population and highlighting the vulnerability of inhabited coastal areas adjacent to major natural drainage routes.

Despite the clear hazard implications, no quantitative sedimentological studies of Stromboli's lahars have been conducted to date. This study provides the first dataset on grain-size distributions of recent lahar deposits, focusing on the events of October 2024 and May 2025. The aim is to document their sedimentological characteristics and to provide baseline parameters for future numerical simulations and hazard assessments.

After a geo-vulcanological overview, this study presents the applied methodologies, including two dedicated field campaigns with sample collection and laboratory analyses, followed by the presentation of results and their comparison with literature data to classify the deposits and detect the source material.

Table 1. Rainfall characteristics associated with recent lahar-triggering events at Stromboli. The table reports, for each event, the total rainfall duration and cumulative precipitation, together with the duration and intensity of the peak rainfall phase (data from the INGV – Attiva Stromboli station, Fig. 1).

Event	Total duration (hr)	Precip. Accum. (mm)	Peak duration (hr)	Peak Accum. (mm)
August 12, 2022	3:45	67.8	2:00	59.7
October 19, 2024	5:00	25.2	1:15	14.0
May 15, 2025	10:30	35.3	3:00	29.5

2. Geo-volcanological setting

Stromboli Island, the northernmost island of the Aeolian archipelago (Southern Italy), covers an area of approximately 12.6 km² and represents the subaerial portion of a large volcanic edifice that rises nearly 3,000 m above the Tyrrhenian seafloor (Bosman et al., 2009). The island's highest point is the Vancori peak, reaching about 924 m a.s.l. (Fig. 1). One of the most distinctive morphological features is the Sciara del Fuoco, a horseshoe-shaped depression on the northwestern flank, which acts as a major pathway for volcanic material generated by landslides and for lava flows since the Roman age (Pasquaré et al., 1993; Tibaldi, 2001).

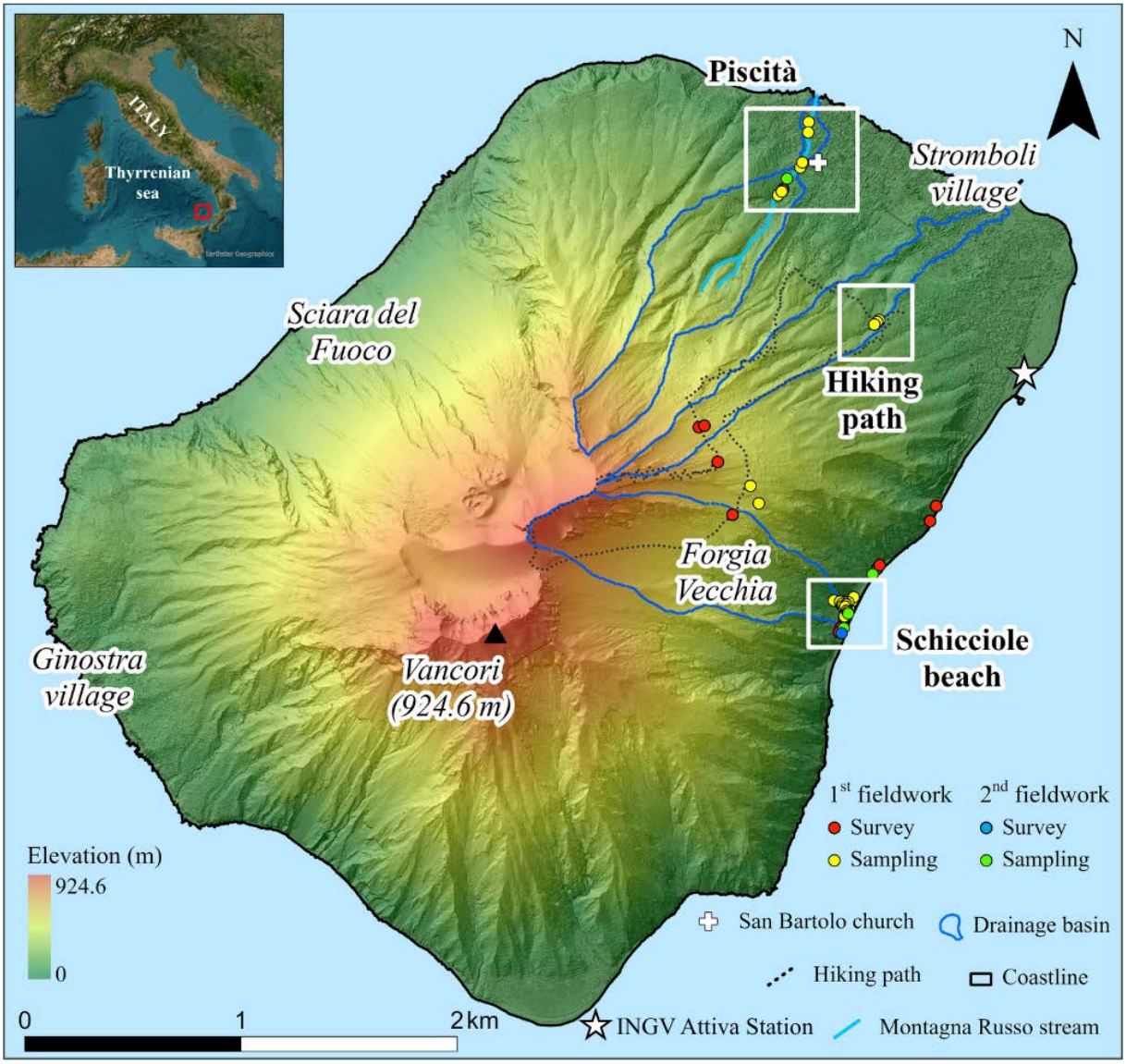

Figure 1. Stromboli island map. Fieldwork stop points are shown: red and blue circles indicate survey locations, yellow and green circles refer to survey locations including also collected samples (from 1 to 3 per site). 1st fieldwork refers to the April 26 to May 1, 2025 campaign, while 2nd fieldwork refers to the June 6, 2025 one. The inset at top left of the figure shows the geographical setting of the island (small red square). White boxes mark the areas detailed in the insets in Fig. 2. In the background, the digital surface model (DSM) of the island (Bisson et al., 2025) superimposed to the shaded relief map.

Volcanic activity is typically concentrated within the summit area on a crater terrace at ~750 m a.s.l., where active vents are hosted in three (NE, Center and SW) main sectors. The typical eruptive style of Stromboli is known as Strombolian activity, which has been ongoing for the past 1000-1500 years (Rosi et al., 2000; 2013). It consists

of mild but persistent explosions generated by the bursting of gas slugs rising through the magma column, usually ejecting scoriae, lapilli and bombs up to tens to hundreds of meters above the active vents, with limited generation of ash. Explosions generally occur at intervals ranging between 5 and 30 per hour (Barberi et al., 1993; Rosi et al., 2013). The Sciara del Fuoco collects most of the scoriae, bombs and blocks produced by the explosions and then channels them down towards the sea (Marsella et al., 2012). The ordinary Strombolian activity is periodically interrupted by lava flows and by more energetic explosive events, classified as major explosions and paroxysms, depending on their magnitude and intensity (Rosi et al., 2013). Coarse tephra erupted during major explosions are generally confined to the summit area, thereby usually affecting only the upper slopes of the edifice, while paroxysms display significantly higher intensities (>10^6 kg/s compared to ~10^4 kg/s for major explosions) and magnitude, involve multiple vents, and generate widespread hazards, including high eruption columns (up to 8-9 km a.s.l.), pyroclastic flows, tephra fallout and ballistic ejecta as far as the coastline and beyond, sometimes generating tsunamis (Bertagnini et al., 2011; Rosi et al., 2013).

3. Methods

To investigate and characterize the lahar deposits, a methodological approach was adopted combining field surveys followed by grain-size analyses. In detail, two dedicated fieldworks were conducted at Stromboli Island to describe and sample lahar deposits. The first survey was conducted between April 26 and May 1, 2025, after the rainfall events that occurred between October 18 and 20, 2024. The second campaign took place on June 6, 2025, following the lahar event of May 15, 2025. The surveys were performed after distinct rainfall events, allowing the associated lahar deposits to be clearly distinguished in the field and sampled separately. The collected samples were subsequently analyzed in the laboratory via mechanical sieving to obtain grain-size distributions and statistical parameters, providing a detailed sedimentological characterization.

3.1 Fieldwork

The areas selected for the field campaigns were Schicciole Beach, Piscità district and other sites along the hiking paths that cross the northeastern flank of the island (Fig. 2). The main drainage basins responsible for channelized runoff and triggering the lahars in the investigated areas are shown in Fig. 1. Schicciole Beach was chosen due to the presence of well-preserved deposits (including the depositional fans) from both the October 2024 and May 15, 2025 events. It was not possible to determine which of the three rainfall days was responsible for the material that reached the beach for the October 2024 deposits. Therefore, these deposits are referred to more generally as belonging to the October 2024 event. No internal stratifications indicative of multiple emplacement phases were observed within the deposits and no eyewitness reports or local accounts are available to clarify

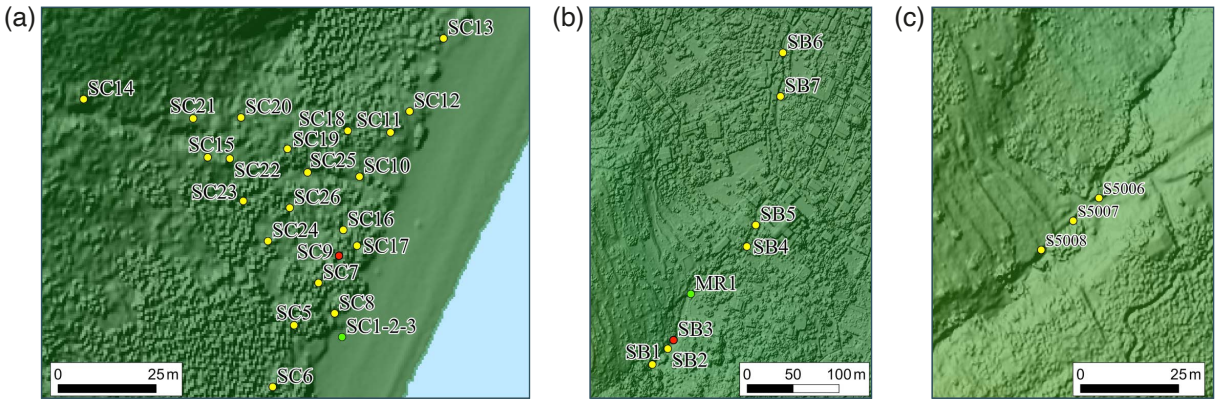

Figure 2. Fieldwork stops maps. The three maps represent the area in the white boxes in Fig. 1: (a) Schicciole Beach; (b) Montagna Russo stream channel directed toward the San Bartolo area; (c) hiking path to the summit. The legend of the stop points is the same as Fig. 1.

this uncertainty. Piscità district was affected by lahars that occurred in October 2024 and May 2025. These flows traveled through the Montagna Russo stream channel and subsequently inundated the surrounding roads close to the church of San Bartolo (Fig. 1). The hiking path was selected as it has been frequently used by volcanological guides and volcanologists (at least before the paroxysm of July 3, 2019; e.g. Andronico et al., 2021). Here, we found lahar deposits considered to be formed during the October 2024 events.

At each investigated site, a detailed field logging of the lahar deposits was carried out. This included the description of deposit thickness, grain-size characteristics, color, internal structures and vertical textural variations.

Figures 1 and 2 show the points observed during the fieldwork, during which a total of 53 locations were surveyed. At specific locations (shown as yellow and green points in Figs. 1 and 2 for the first and second fieldwork, respectively), sampling of materials was also done. In most cases, from 1 to 3 samples were collected at each stop. For the first campaign, a total of 46 outcrops were surveyed, and 45 samples were collected from 32 sites; during the second campaign, 7 samples were collected from 5 sites. Table 2 summarizes the collected samples with the indication of their ID, area, X and Y UTM coordinates and a short description.

The main objective for sampling the lahar deposits was to characterize the grain-size variability within each layer. In some cases, a single sample was sufficient; conversely, where vertical variations were evident from the base to the top of the deposit (in terms of grain-size, color, sorting, etc.), multiple samples were collected at different heights to account for these variabilities.

The geographic location of each sampling site was recorded using a Garmin GPSMAP 62stc handheld GPS device, with a planimetric accuracy of approximately ±1.5 m under optimal signal conditions. This device enables the creation of waypoint files containing detailed geospatial and contextual metadata, including the sample ID (unique sample code) X, Y, Z coordinates and, when necessary, photographs of the sampling location.

Table 2. List of the collected samples during the fieldworks. The metric coordinates of X and Y are in the WGS 84 UTM N33 system.

ID	Area	X	Y	Description
SC5	Schicciole Beach	520028.0	4293355.4	Collected at the intersection with an erosional channel
SC6	Schicciole Beach	520022.6	4293339.7	Lateral part of the October 2024 fan
SC7a	Schicciole Beach	520034.2	4293366.2	Base of the October 2024 fan (collected 45 cm above the reeds level)
SC7b	Schicciole Beach	520034.2	4293366.2	Sample collected 60 cm above SC7a
SC7c	Schicciole Beach	520034.2	4293366.2	At the top of the October 2024 fan
SC8	Schicciole Beach	520038.3	4293358.4	Deposit sampled above a boulder (Fig. 5b)
SC10a	Schicciole Beach	520044.7	4293393.2	Base of the October 2024 fan (collected 65 cm above the reed level)
SC10b	Schicciole Beach	520044.7	4293393.2	Sample taken ~50 cm above the top of SC10a; between the two levels there is ~40 cm of block-rich facies, located ~80 cm above the reed base. Presence of a boulder measuring 110 × 75 cm
SC10c	Schicciole Beach	520044.7	4293393.2	At the top of the October 2024 fan
SC11a	Schicciole Beach	520052.6	4293404.4	Base of the October 2024 fan (collected 32 cm above the reed level)

ID	Area	X	Y	Description
SC11b	Schicciole Beach	520052.6	4293404.4	Sample taken immediately above SC11a
SC11c	Schicciole Beach	520052.6	4293404.4	At the top of the October 2024 fan
SC12a	Schicciole Beach	520057.4	4293409.7	Base of the October 2024 fan
SC12b	Schicciole Beach	520057.4	4293409.7	Sample taken above the top of SC12a
SC12c	Schicciole Beach	520057.4	4293409.7	At the top of the October 2024 fan
SC13 bottom	Schicciole Beach	520066.0	4293428.3	Lateral part of the October 2024 fan (basal)
SC13 top	Schicciole Beach	520066.0	4293428.3	Lateral part of the October 2024 fan (top)
SC14	Schicciole Beach	519974.5	4293412.9	Near the erosion/deposition boundary
SC15	Schicciole Beach	520006.0	4293398.1	Sample from a stratified layer beneath a 35 cm thick lobe
SC17a	Schicciole Beach	520044.0	4293375.6	Basal layer of 15 cm of a brownish deposit (likely from June 2024 event)
SC17b	Schicciole Beach	520044.0	4293375.6	Base of the October 2024 flow (the deposit here is channelized)
SC17c	Schicciole Beach	520040.5	4293379.6	On the top of the fan (20 cm below the surface)
SC18	Schicciole Beach	520041.7	4293404.8	At the top of the October 2024 fan
SC19	Schicciole Beach	520026.3	4293400.2	At the top of the October 2024 fan
SC20	Schicciole Beach	520014.5	4293408.2	At the top of the October 2024 fan
SC21	Schicciole Beach	520002.3	4293407.9	At the top of the October 2024 fan
SC22	Schicciole Beach	520011.7	4293397.7	At the top of the October 2024 fan
SC23	Schicciole Beach	520015.1	4293387.0	At the top of the October 2024 fan
SC24	Schicciole Beach	520021.4	4293376.8	At the top of the October 2024 fan
SC25	Schicciole Beach	520031.5	4293394.2	At the top of the October 2024 fan
SC26	Schicciole Beach	520026.9	4293385.2	At the top of the October 2024 fan
SC_1505125_1	Schicciole Beach	520040.2	4293352.4	On the top of a May 2025 fan
SC_1505125_2	Schicciole Beach	520040.2	4293352.4	Sampled below SC_1505125_1
SC_1505125_3	Schicciole Beach	520040.2	4293352.4	Sampled below SC_1505125_2. Basal matrix rich in blocks that lies directly on the beach

ID	Area	X	Y	Description
SC_1505125_4	Schicciole Beach	520153.0	4293535.2	Total sample on a May 2025 fan
SC_1505125_5	Schicciole Beach	520020.1	4293285.1	Total sample on a May 2025 fan
SB1	Piscità	519715.6	4295288.8	Near the erosion/deposition boundary, with presence of blocks ~6-7 cm in size
SB2	Piscità	519732.3	4295305.9	Slightly downstream from SB1
SB4 bottom	Piscità	519818.4	4295416.8	Basal layer of the deposit downstream
SB4 top	Piscità	519818.4	4295416.8	Sampled above SB4 bottom
SB5	Piscità	519828.2	4295440.2	Downstream deposit
SB6	Piscità	519857.5	4295627.2	Sampled near Riposto street
SB7	Piscità	519854.9	4295579.8	Sampled near Riposto street
MR_1505125_1	Piscità	519757.3	4295365.3	Sample of the channel bed, near the intersection with the road
MR_1505125_2	Piscità	519757.3	4295365.3	Pumice layer above MR_1505125_1
S5004	Hiking path	519626.3	4293863.0	Sample from a small flow. The material is similar to that of Schicciole deposits
S5005	Hiking path	519587.9	4293944.1	Source material of the Schicciole lahars
S5006a	Hiking path	520183.6	4294710.8	Deposits from August 2022, found along the lower section of the ascent trail. Cemented road visible at the base
S5006b	Hiking path	520183.6	4294710.8	Sampled above S5006a
S5006c	Hiking path	520183.6	4294710.8	Sampled above S5006b; possibly from the October event
S5007	Hiking path	520173.4	4294701.8	Slightly above sample 5006, a single layer resting on lava. Between the deposit and the lava, a pumice level is present
S5008	Hiking path	520160.6	4294690.2	Near the erosion/deposition boundary. Same material of S5007

3.2 Laboratory Analyses

The 52 collected samples were analyzed at the Laboratory of Volcanology of the Istituto Nazionale di Geofisica e Vulcanologia (INGV) in Pisa, with the specific aim of obtaining detailed granulometric parameters for the characterization of lahar deposits. The analyses were carried out through mechanical dry sieving, following standard procedures widely employed in volcanological and sedimentological studies. Prior to the analyses, all samples were dried at 60 °C for at least 24h to eliminate residual moisture. Grain-size analyses were performed

using a mechanical sieve shaker (Giuliani IG/1) equipped with a stack of nested columns of half-φ interval sieves, ranging from −2 φ to 5.5 φ ($\varphi = -\log_2 d$, where d is grain diameter in mm). For the coarser fractions, −3 φ and −4 φ sieves were additionally used to improve characterization. Before the sieving procedure, each sieve was individually weighed to obtain its tare, which was later subtracted from the final measurements to ensure accuracy.

During the grain-size analyses, the sieves were stacked in the mechanical shaker and subjected to two successive 5-minute shaking sessions. After the first session, the entire stack was rotated by 90° both to ensure a more uniform distribution of the sediment across the mesh surfaces, and to improve the efficiency of the grain-size separation.

At the end of the shaking process, each sieve containing the retained material was weighed. All values were recorded in spreadsheets and statistical parameters were calculated. For each sample, cumulative grain-size curves and weight-percentage histograms were generated. From these datasets, graphic parameters such as mean grain-size, median, standard deviation (sorting), skewness and kurtosis were calculated, following standard statistical procedures for sedimentological data. Skewness was used to describe the degree of asymmetry of the grain-size distribution curves, providing information on the relative enrichment in fine or coarse fractions, whereas kurtosis (peakedness) compares sorting in the central portion of the distribution with that in the tails. The grain-size classification adopted was that of Udden-Wentworth (Udden, 1914; Wentworth, 1992). This is based on the dominant grain-size fraction and is commonly employed for the classification of lahar deposits (Capra et al., 2010; Lavigne et al., 2000; Manville et al., 2013; Scott et al., 1995).

4. Results and Discussion

4.1 Field data and deposit characteristics

The results of the field observations and the main characteristics of the lahar deposits on Stromboli Island are presented in this section, discussing separately the 3 investigated areas: Schicciole Beach, Piscità and the hiking path on the northeastern flank of Stromboli. At Schicciole Beach and Piscità, deposits related to both October 2024 and May 2025 lahar events were identified, whereas along the hiking path, only deposits associated with October 2024 events were recognized. After the fieldwork, the collected waypoints were transferred to a computer using Garmin BaseCamp software, which facilitated the organization and preliminary visualization of the georeferenced data. Subsequently, the data were imported into a GIS environment (ArcGIS Pro software – ESRI platform), where the sampling locations were integrated into a spatial database.

4.1.1 Schicciole Beach

Schicciole is a beach located on the southeastern coast of Stromboli (Fig. 1 and Fig. 2a), whose width can vary by several meters depending on the interaction between the continuous supply of sediment along the slope and continuous marine erosion (Fig. 2a). This area was chosen due to the presence of well-preserved deposits (including the depositional fans) from both the October 2024 and May 2025 events. The beach lies downslope from the Forgia Vecchia area, a sector highly susceptible to gravitational remobilization, especially during intense rainfall events. Samples from Forgia Vecchia source material were also sampled. This deposit is considered to be the primary supply for the flows that later reached the Schicciole Beach. Lahars transport material down from the upper slopes, which then deposits directly on the beach, reaching the sea during the most intense lahar episodes. Since the distal deposits are directly affected by marine erosion, timely sampling is essential to characterize the entire deposit. At the time of our first campaign (April 26-May 1, 2025), this area featured at least three depositional fan-shaped lahar deposits (Fig. 3a). The central one (Fig. 3b) is one of the most preserved depositional fans and is attributed to the October 2024 rain events by the presence of a reed layer used as a basal stratigraphic marker. The attribution of the other two depositional fans to the October 2024 events is less certain due to the absence of the reed layer. In detail, the southernmost fan (left side in Fig. 3a) is characterized by more eroded and weathered material, overlain by reeds, indicating deposition before October 2024. Conversely, the deposits of the northernmost depositional fan (right side in Fig. 3a) display characteristics (mainly color and grain-size) comparable to those of the central fan, suggesting a possible association with the October 2024 event; however, the lack of the reed layer makes the event attribution uncertain.

Figures 3, 5 and 6 show stratigraphic features of the main distal deposit fan of October 2024 lahar, which is the largest, with an approximate width of ~85 meters and a length of ~109 meters. The maximum measured thickness of the deposit, in its central portion, is approximately 3.5 meters (Fig. 5d). To distinguish this deposit from older events, a basal layer characterized by a line of almost continuous bent reeds was used as a reference (Fig. 5a). As shown in the figures, these reeds typically grow on top of previous deposits, and prior to the October 2024 events, they entirely covered the area (Fig. 4).

Figure 3. Schicciole Beach area after October 2024. (a) Views of the beach: white dashed lines highlight the depositional fans, blue lines are the drainage axes correlated to the fans and white circle indicates the Forgia Vecchia area (b) Detailed view of the central fan. Photos by D. Andronico and R. Gianardi.

The October 2024 central fan deposit overlies a succession composed of two distinct deposits, one forming the beach substrate and the other associated with previous lahar events. In detail, the beach substrate has a thickness of 10-15 cm, and is mainly composed of rounded clasts of scoriae and lavas (Fig. 6c). Overlying the beach substrate are older lahar deposits, with thicknesses ranging from several tens of centimeters to approximately 1 meter. These deposits have variable grain-size, including centimetric to decimetric rounded clasts, as well as compact, sandy layers; inside these deposits, roots are commonly found. At the contact with the central, October 2024 lahar deposit, a ~5 cm thick layer of brown ash can be observed mainly in the central part (Fig. 6d), likely associated with minor lahar events that occurred around June 2024, immediately after the landslide events along the Sciara del Fuoco.

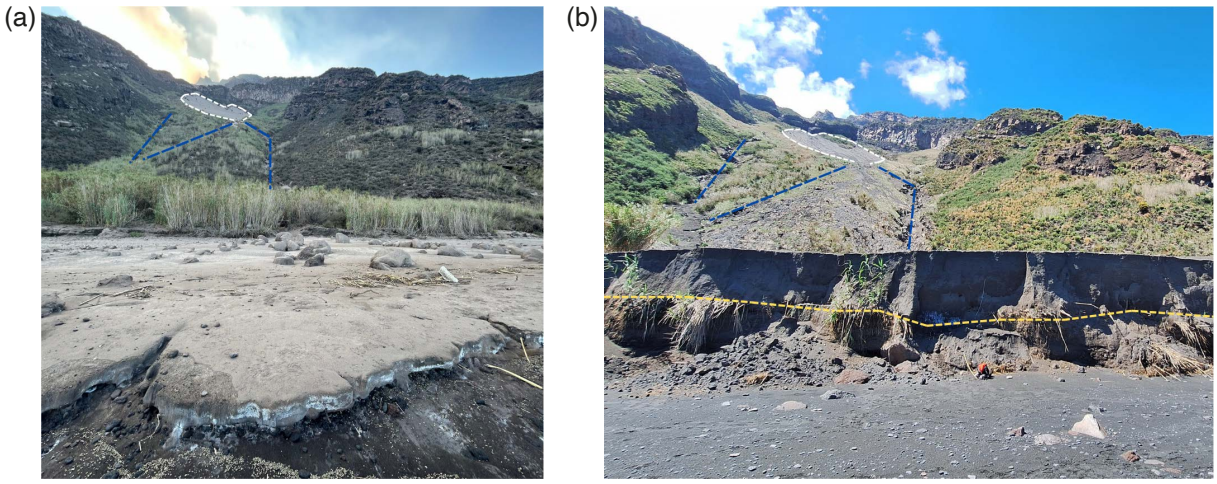

Figure 4. Comparison between the Schicciole Beach area before (a) and after (b) the October 2024 lahars. Photo in (a) was taken in June 2024 and shows the initial remobilization processes of the material emplaced during the lahars of June 2024 (for scale purposes the thickness of the deposit is 10 cm in its front), (b) was taken on April 27, 2025 during the first fieldwork (for scale purposes the backpack is 30 cm tall). White lines highlight the Forgia Vecchia area, blue lines are the drainage axis and the yellow line is the limit of the reed layer. Photos by M. Pistolesi and R. Gianardi.

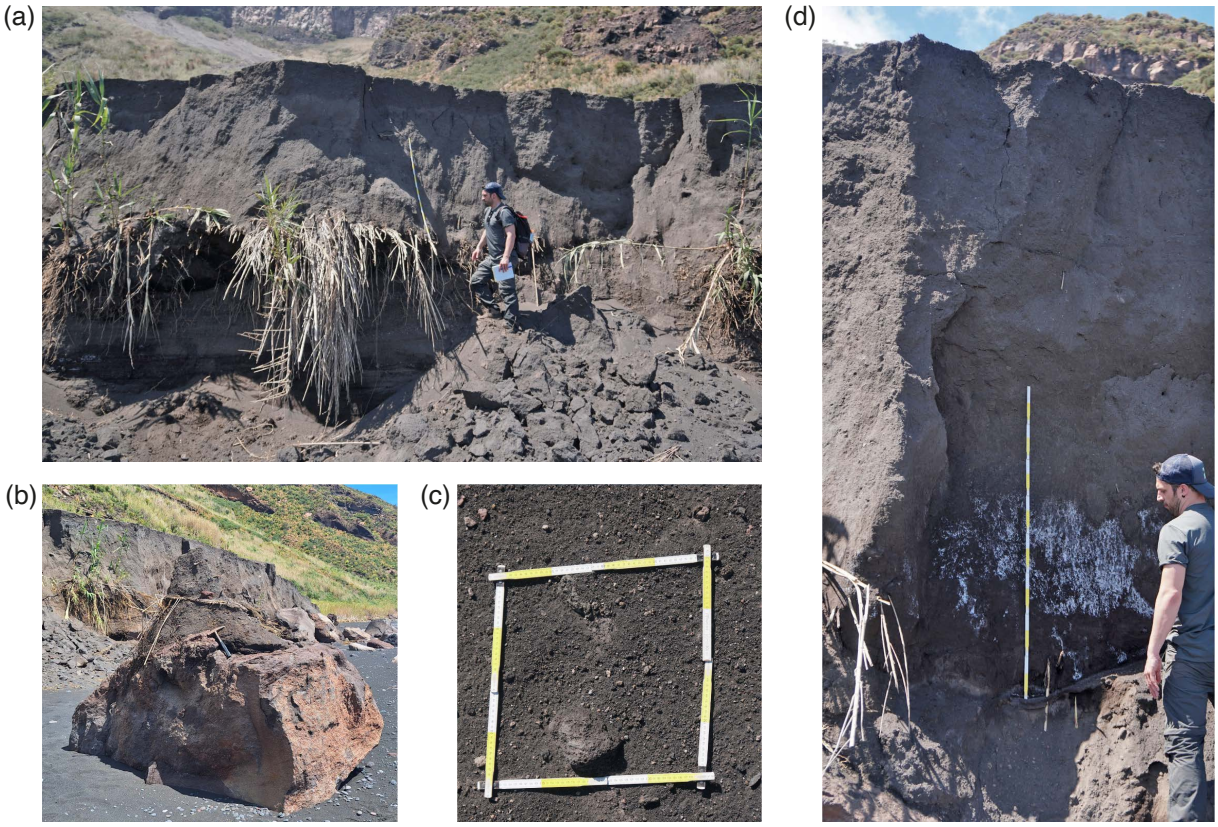

Figure 5. Deposit features at Schicciole Beach, during the first fieldwork on the main, central lahar: (a) overview of a proportion of the lahar front, where a line of bent reeds is visible; (b) distal boulder covered by the October 2024 deposit; (c) surface at the roof of the thick fan-shaped lahar deposit; (d) detail of the thickness and general facies of the deposit. Photos by R. Gianardi and D. Andronico.

The reed layer overlies the previous lahar deposits (Fig. 5a), separating the October 2024 flow from older deposits and can be traced continuously across the full width of the fan.

The October 2024 fan deposit is massive, with no clear evidence of stratification and characterized by a finer overall grain-size (dominance of sand- to pebble-sized material), with sparse, centimeter-scale clasts. The deposit is black to dark brown, typical of the pyroclastic products of Stromboli. Based on outcrop-scale observations, the deposit suggests deposition from a high-concentrated flow. These features are consistent with hyperconcentrated-flow deposits, which typically lack the matrix-supported fabric of debris flows and do not display the stratification commonly observed in fluvial deposits.

The erosion/depositional boundary (Fig. 6b, SC14 in Fig. 2a) can be traced upslope at a distance of around 100 meters from the distal central part of the fan along the Forgia Vecchia channel. In this area, the deposits tend to be coarser with more centimeter-scale clasts and laminations are present in the upper part (15-20 cm) (Fig. 6a).

The fan's front and the older deposits are vertically cut at the beach front, approximately at the break in slope. This suggests that these deposits underwent erosion over time, primarily due to the sea's action on the narrow beach (only a few meters wide), but also likely influenced by other morphological and meteorological factors. The hypothesis of sea erosion is justified by the presence of a multi-meter sized boulder (up to 3 m in maximum axis; Fig. 5b, SC8 in Fig. 2a) transported downslope and located near the sea, over which the lahar deposit is preserved, including the reed layer. The elevated position of this deposit on top of the boulder avoided its direct wave erosion, while the remaining deposits were eroded.

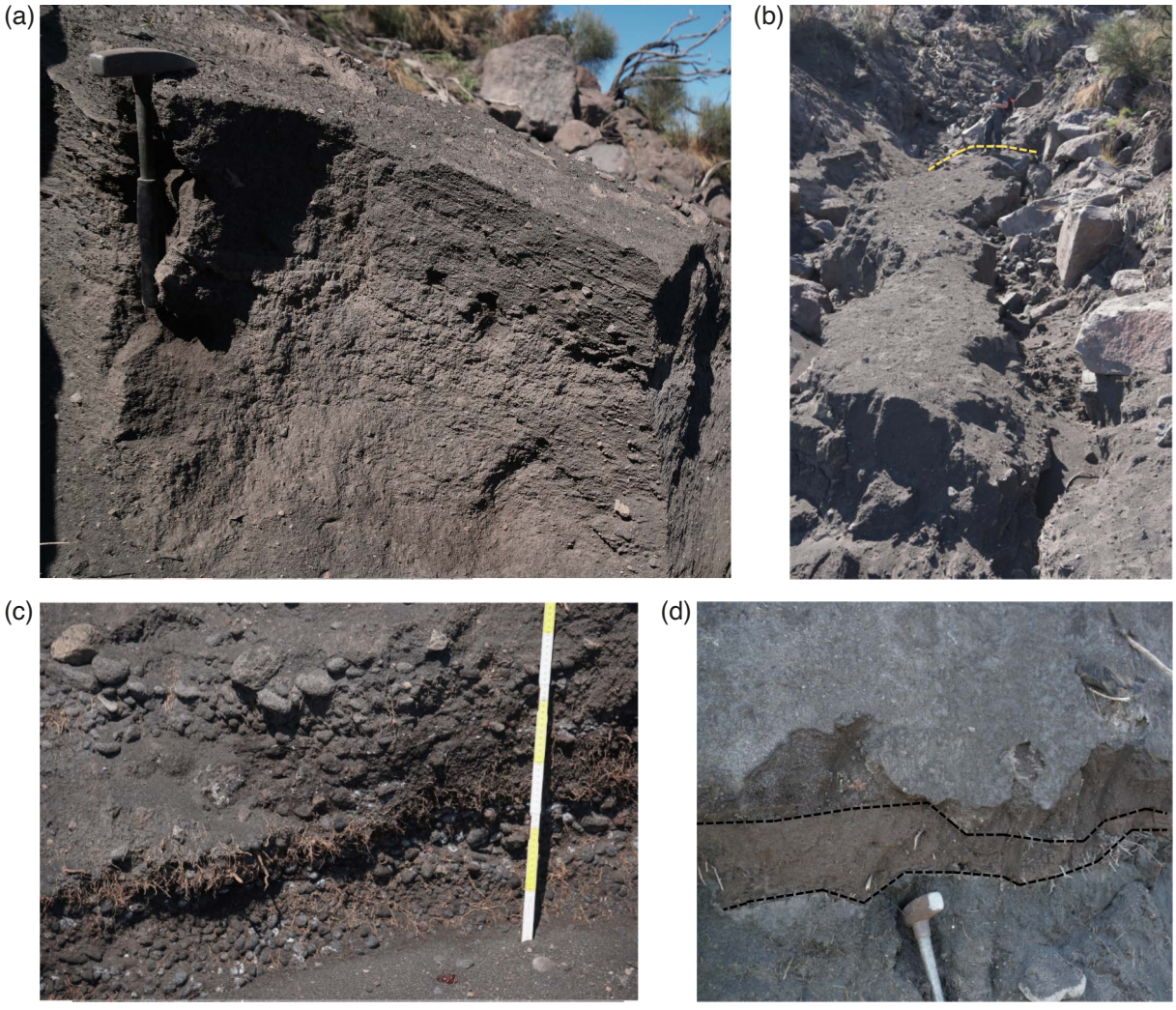

Figure 6. Deposit features of the October 2024 lahar: (a) and (b) first deposit near the erosion/deposition limit (yellow line); (c) basal rounded scoria/pumice layer (white line is the limit with the beach substrate); (d) brown ash layer within the deposit (highlighted with the black lines). Photos by R. Gianardi and D. Andronico.

Following the intense rains of May 15, 2025, at least four additional small deposits formed on the Schicciole Beach (Fig. 7a, b, c), and were observed approximately three weeks later during the June 2025 field campaign. The timing of the two different field campaigns allowed to clearly distinguish, in the field, the deposits associated with the October 2024 and May 2025 rainfall events. The more recent deposits, in fact, consisted of small lahars that had incised both the older lahar deposits or, in one case, run along their lateral edge, forming small, symmetrical alluvial fans that spread out at the foot of the October 2024 deposits (Fig. 8). The first fieldwork (April 26 to May 1, 2025) allowed to observe that the October 2024 deposits were still intact and did not exhibit evidence of incision prior to the May 15 event. The observed incision features are therefore interpreted as having formed during the May 15 event.

These fans exhibited their maximum thickness at the center (i.e. approximately along the propagation direction), from 30 to 80-100 cm (Fig. 7), decreasing laterally toward the edges of the fan. Moving from N to S along the beach, we found the thinnest deposit (30 cm) just 20-30 m after the northernmost depositional fan of Fig. 3a. This small lahar was laminated by alternating centimeter-thick layers of variable grain-size bearing ash particles (from fine to coarse). Moving forward, the second lahar (SC1-2-3 in Fig. 2a) had flowed over and carved the southernmost side of the October 2024 deposit. It was featured by a ~40 cm-thick basal layer laying directly above the beach surface, including numerous blocks, some of them up to decimetric size and more. This layer then graded into an overlying layer (~60 cm thick) very similar to the previous, 2025 thinner lahar deposit. The base of the large boulder of the October 2024 deposit (Fig. 5b) was surrounded by this flow for almost half of its height (Fig. 7a). A third deposit (Fig. 7b) had carved the southernmost fan emplaced before October 2024 (left side in Fig. 3a). It was highly

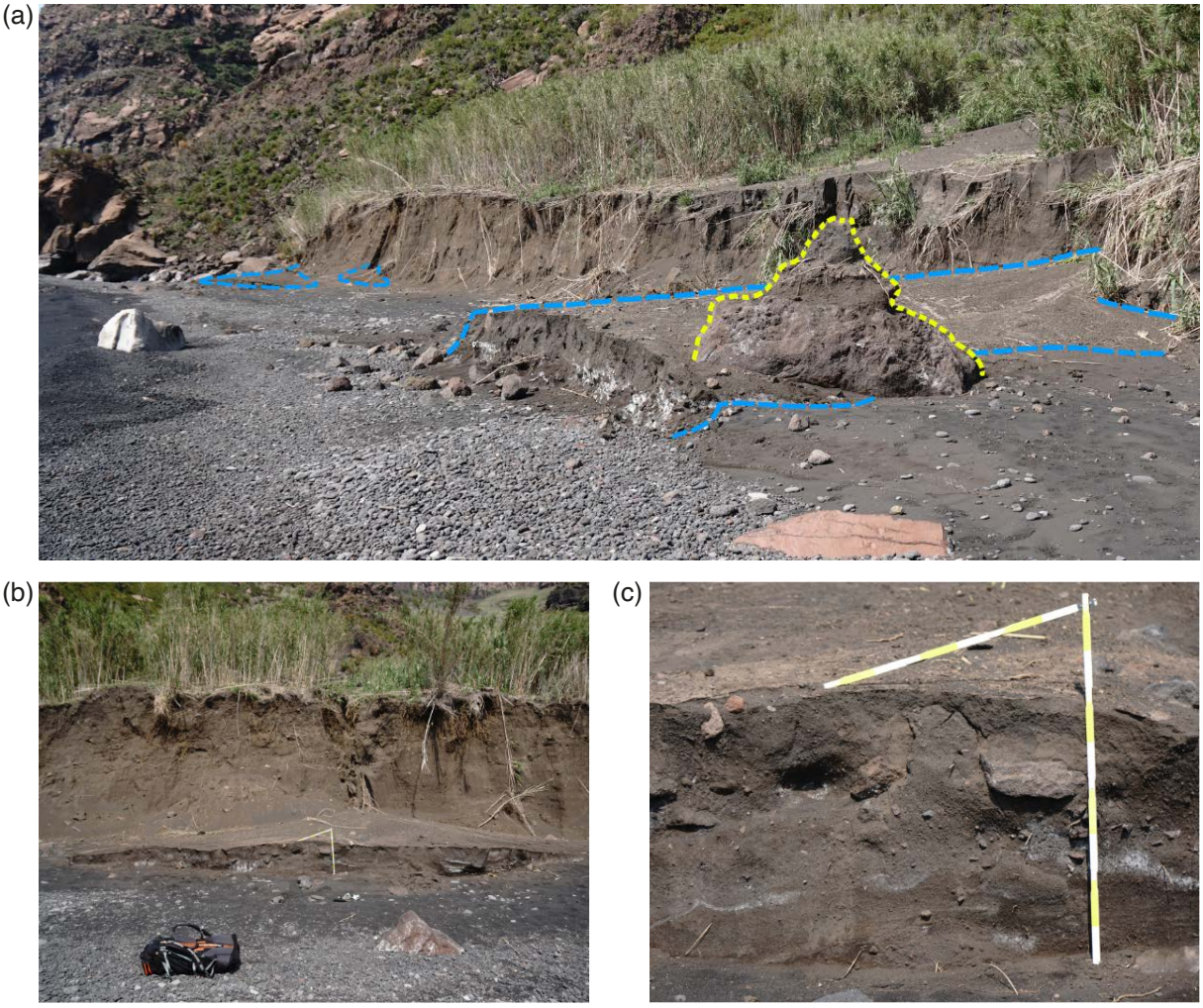

Figure 7. Depositional features of the May 2025 lahars: (a) the large October 2024 boulder (yellow dashed line) surrounded by the May 2025 deposits; the blue dashed lines highlight 3 lahar deposits in sequence going south along the beach; (b) overview and (c) detail respectively, of the 2025 thicker lahar deposit of a depositional fan. Photos by D. Andronico.

chaotic with a maximum thickness of more than 60 cm, with the left, southern half rich in blocks (up to 50 cm in size) and the right, northern half more massive (Fig. 7c). Finally, close to south end of the beach, the last May 2025 lahar deposit (~40 cm thick) appeared similar to those associated to the October 2024 event, being relatively massive and homogeneous in terms of particle grain-size, and composed of dark brown sand with scattered pluri-centimetric clasts. It was also evident that the May 2025 deposits had initially reached the sea, but the continuous action of the marine waves had already eroded their distal portions (Fig. 7a and b). This process likely completely eroded even smaller deposits than those observed.

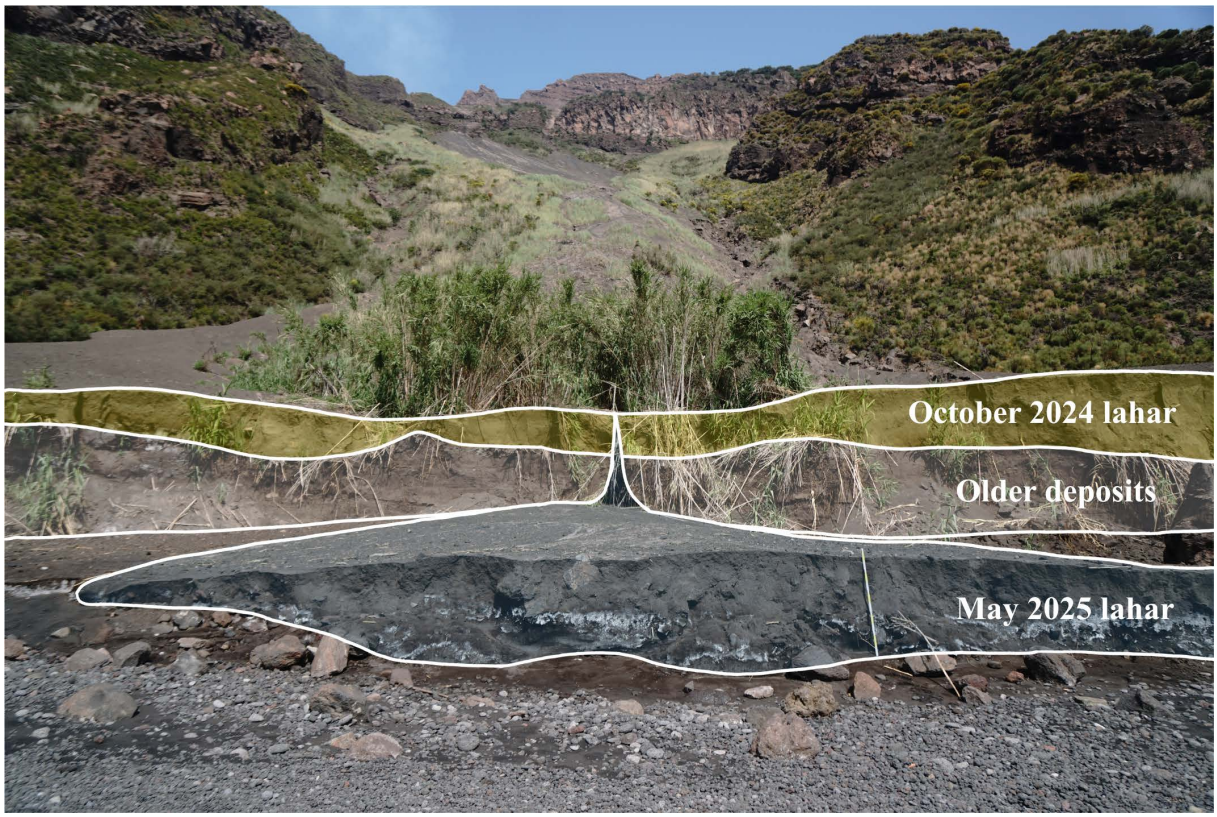

Figure 8. Stratigraphic relationship between the lahar deposit at Schicciole Beach after the May 15, 2025 events. In chronological order: older pre-2024 deposits (white), overlain by the October 2024 lahar deposits (yellow). The sequence is subsequently cut by the depositional fans formed during the May 2025 event (blue). Photo by D. Andronico.

In addition to fieldwork, Pleiades satellite images acquired in June 5, 2025 and covering approximately 180 km^2 were used for mapping the lahar deposits (Fig. 9). The images, acquired after the lahar event and the following fieldworks, allowed a spatial characterization at high spatial resolution of the central fan emplaced on the Schicciole Beach (Fig. 3b).

The Pleiades high-resolution data are acquired by panchromatic and multispectral sensors onboard the polar orbiting Pleiades 1A, Pleiades 1B and Pleiades NEO satellites. The sensors work in the visible (VIS) and the near-infrared (NIR) spectral range. The panchromatic sensor acquires images at 50 cm ground resolution while the multispectral sensor acquires images at 2 m of ground resolution (Palaseanu-Lovejoy et al., 2019). The Schicciole central fan spatial extent has been identified by using the method proposed in Spinetti et al. (2009), resulting in an area of approximately 0.03 km^2.

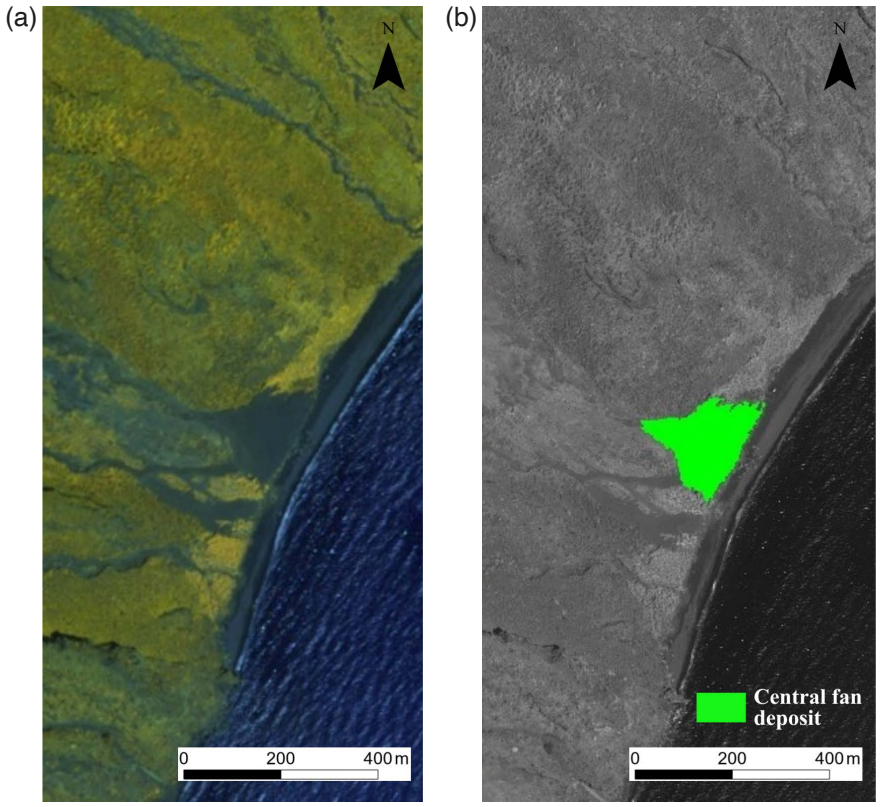

Figure 9. Pleiades high resolution optical data acquired on June 5, 2025: (a) RGB composition of the Schicciole beach area; (b) Schicciole central depositional fan identified in the panchromatic band.

4.1.2 Piscità

Piscità is a residential district located in the northern part of the Stromboli village (Fig. 2b). This area includes the channel of the Montagna Russo stream, near the San Bartolo church, which has played a major role in the remobilization of debris and the formation of lahars in recent years, including the studied events of October 2024 and May 2025. In fact, following intense precipitations, this channel rapidly fills with remobilized volcanic material, often resulting in destructive consequences for the inhabited area. Local accounts report that the Montagna Russo channel has been repeatedly affected by remobilization processes since 2022, including minor flows, which demonstrate its persistent susceptibility to lahar activity. A critical point for the lahar hazard occurs at an elevation of approximately 30 m a.s.l., where the channel passes beneath the road (Fig. 10). Here, when lahars descend through the torrent, their high velocity and large sediment load commonly exceed the channel's capacity. As a result, the flows overflow onto the road surface, with the sediment load following the local slope as it propagates downslope along Riposto Street. However, the lahars also inundate the houses of the Piscità area, affecting areas both downstream and significantly upstream of the point where the channel intercepts the road. This process significantly increases the hazard for the residential area, where numerous homes are severely threatened by the lahars. During the October 2024 events, for example, also metric blocks were transported in Piscità (Fig. 11b), proving the considerably destructive potential of the flow.

At the time of the first survey, the Montagna Russo channel had already been partially cleared using excavators, and most of the removed material was accumulated along its flanks (Fig. 10a). Nevertheless, we were able to sample undisturbed portions of the lahar filling the channel, including the first deposit after the erosion/deposition boundary and on specific curved segments where the flow deceleration had promoted sediment accumulation. During the first survey, the most distal deposits were identified about 400 meters downstream with respect to the erosion/deposition boundary, along Riposto Street, with deposits reaching a maximum thickness of ~80 cm (Fig. 11c). At the time of the second survey, after the May 2025 event, the channel had not yet been cleared (Fig. 10b), allowing direct observation and measurement of lahar deposits in situ. In this case, the thicknesses ranged between 50 and 60 cm.

Figure 10. Lahar in the Piscità district, on the intersection with the road, following the October 2024 (a) and May 2025 (b) events. Note that, at the time of the first survey, the channel was cleared from the debris. Photos by R. Gianardi and D. Andronico.

In the Piscità area, samples were collected along the Montagna Russo stream (Fig. 11a) as well as further downstream (Fig. 11c), following the course of the stream, for both the October 2024 and May 2025 deposits.

The proximal deposit of the October 2024 lahar, close to the erosion/deposition boundary (SB1 in Fig. 2b), is characterized by a dark color, a sandy grain-size and with no internal stratification. On top of the deposit porphyric rock blocks occur, up to ~50 cm in size. These clasts are from older lavas, probably referable to the Roman age San Bartolo lava units emplaced around the area and are also present within the deposit, as fragments with sizes of 6-7 cm. Moving downstream along the Montagna Russo channel, the deposit remains similar but more brownish in color, reaching thicknesses up to 80 cm. In correspondence with channel bends (SB4 in Fig. 2b), the dry surface of the deposit exhibits longitudinal layerings and the deposit appears subdivided in two parts. However, no clear difference in color, texture or grain-size were identified inside the deposit. In the distal sector (SB6 and SB7 in Fig. 2b), the lahar deposit is characterized by a thickness of ~60 cm and a deeper brownish color. As observed upstream, the deposit is massive, with no internal stratification. These characteristics are consistent with hyperconcentrated-flow deposits, although the presence of large, isolated blocks transported at the surface and within the deposit indicates locally higher sediment concentrations and energy conditions, especially in the proximal sector, probably related to the confinement of the flow within the Montagna Russo channel.

The May 2025 lahar that affected the Piscità area had a more significant impact than the October 2024 event. Nevertheless, it exhibited a similar capacity to transport pluri-decimetric boulders through the Montagna Russo channel, spreading them beyond the road intersection (Fig. 10b). The resulting deposit formed a sandy layer ranging from a few centimeters to several decimeters in thickness along the channel bed and margins, overlying previous lahar deposits. A sample of the fine-grained deposit was collected from the channel bed (MR1 in Fig. 2b), several tens of meters downstream of the erosion/deposition boundary, where the layer reached a thickness of approximately 4-5 cm (Fig. 2b).

Figure 11. Evidence of the October 2024 lahar in the Piscità district: (a) deposition along the bends of the channel; (b) a metric-sized boulder that transported downslope following the October 2024 lahar; (c) deposit parallel to Riposto Street. Photos by R. Gianardi and D. Andronico.

4.1.3 Hiking path

The hiking path is a well-established loop trail used before the 2019 paroxysms by volcanological guides and tourist groups to ascend to the summit area of Stromboli (specifically to Pizzo Sopra La Fossa, Fig. 1 and Fig. 2c) and to descend approximately at the same starting point. It runs along the northeastern flank of Stromboli, including a few hundred-meters section travelling at approximately 500 m a.s.l. during its descending portion. Along this relatively flat part of the path, small flows formed during the remobilization of low volumes of tephra are common on this side of the volcano. However, due to the intense erosion and the highly dynamic nature of the area, these flows are constantly buried by additional tephra fallout, making them no longer preserved and thus difficult to identify.

At the beginning of the path (~115 m a.s.l.), the drainage channel crossing the trail was affected by remobilized material from the October 2024 event (Fig. 12). This drainage incision channeled the lahar leading the flow to cut across the trail. At this site, the erosion/deposition boundary was clearly distinguishable and was sampled (Fig. 12a, S5008 in Fig. 2c). The distance between the boundary and the last sampled outcrop is about 30 m, with a maximum observed thickness of ~50 cm. Beyond this point, the deposit could not be further traced as it descended into a small escarpment. The deposit appeared generally fine-grained: at the base, a brownish, coarser layer was observed, containing a basal horizon of centimetric pumice clasts, whereas the upper part was

darker (almost black) and noticeably finer. This basal layer could be the remains of some previous lahar events, while the upper layer resembles the characteristics of the October 2024 event (Fig. 12b and c). The absence of clear internal stratification within the upper layer, together with its homogeneous texture, is consistent with hyperconcentrated-flow dynamics. However, the presence of a basal coarser layer, possibly related to previous events, indicates a degree of vertical variability and suggests that these deposits may reflect successive remobilization phases under varying flow conditions.

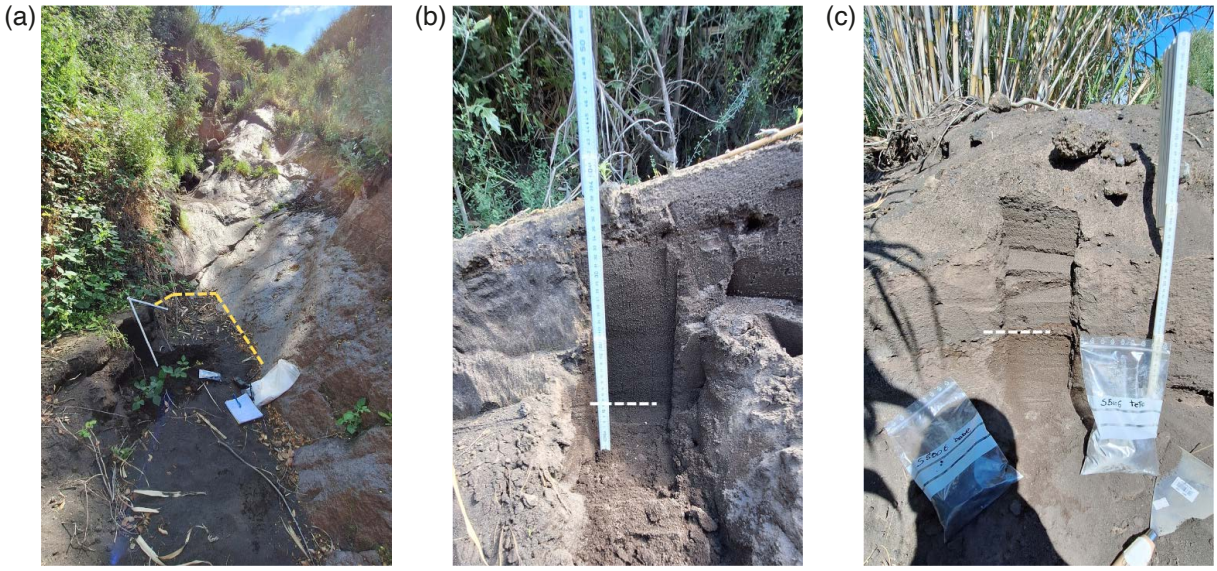

Figure 12. Lahar deposits along the hiking path. (a) Erosion/deposition limit (highlighted with the yellow line); (b) sampling of proximal facies; (c) sampling of the distal facies. White lines in b and c separates the basal horizon from the upper part of the deposit. Photos by R. Gianardi.

Along the path toward the southeastern summit area, at an elevation of approximately 450 m a.s.l., the remains of an older lahar flow were identified (Fig. 13). This deposit, partially buried beneath more recent pyroclastic fallout, was also sampled and provides further evidence of the recurrent remobilization processes affecting the upper slopes.

Figure 13. Sampling of an old lahar at 450 m a.s.l. along the hiking path. Photo by R. Gianardi.

4.2 Grain-size analyses

This section presents the results of the grain-size analyses, which are fundamental for constraining the type and nature of the studied lahars and providing key insights into their sedimentological characteristics and flow dynamics. The dataset is structured according to the three investigated sectors: Schicciole Beach, Piscità, and the hiking path. Specifically, for the deposits of the October 2024 events, due to the larger amount of collected samples, it was possible, for each area, to derive base-to-top variability for the grain-size. At the Schicciole Beach, the presence of the well-preserved depositional fan from the October 2024 event allowed it to conduct a more detailed characterization. In this case, the grain-size distributions were analyzed by considering the variability of the deposit in the longitudinal (Fig. 14a), lateral (Fig. 14d) and vertical dimensions. In Piscità and along the hiking path, the depositional fans could not be identified and the sampling was therefore limited to the exposed deposits along the channel and the volcanic slopes, respectively. For these two sectors, the deposits of October 2024 events were characterized longitudinally (Fig. 14b and c), focusing on downstream trends variations.

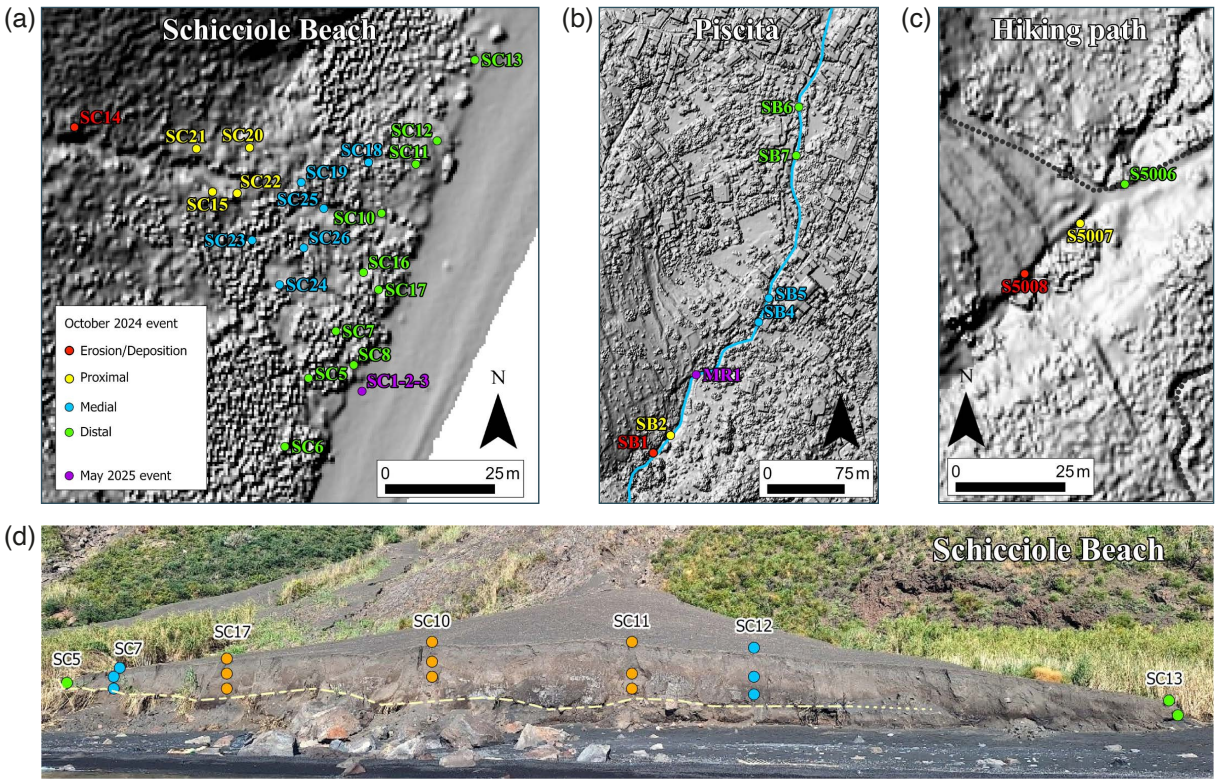

Figure 14. Spatial distribution of sampling points for the lahar deposits. Longitudinal classification of samples from proximal to distal sectors are shown in (a) for Schicciole Beach, (b) for Piscità and (c) for the hiking path. (d) Cross-sectional classification of samples collected along the front of the October 2024 lahar deposit at Schicciole Beach (from the lateral to the central portion): green points are lateral samples, light-blue are median samples and orange are central samples. The yellow dashed line represents the reed layer in order to highlight the base of the October 2024 deposit.

The overall dataset of samples is characterized by a mean mode of $\varphi = 2$, corresponding to the 0.25-0.355 mm size fraction (Fig. 15), which indicates a dominance of sand within all the lahar deposits.

Figures 16 and 17 present the cumulative grain-size curves of the deposits, highlighting the longitudinal variability for all the investigated areas and the lateral variability for the Schicciole Beach deposits.

At the Schicciole Beach, the deposits related to the October 2024 lahars, in the proximal and central portions of the fan are overall coarser than those in the distal or lateral zones (Fig. 16a-b). In particular, the sample collected near the erosion/deposition boundary shows the coarsest sizes for the presence of decimetric clasts which deposited early. These clasts display a heterogeneous composition with both dense (likely lava fragments) and scoriaceous clasts.

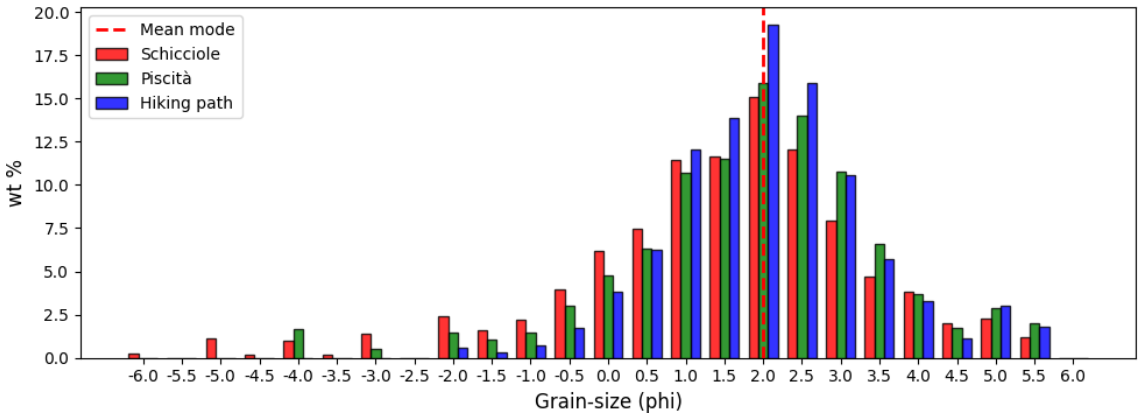

Figure 15. Diagram of the mode distribution for the analyzed samples. For clarity, the data are grouped into the three areas (Schicciole, Piscità, and Hiking path). Within each area, the weight percentage values correspond to the mean for each φ size class, averaged over all samples belonging to that group. The dashed vertical line represents the average of the modal values of the samples of the three studied areas.

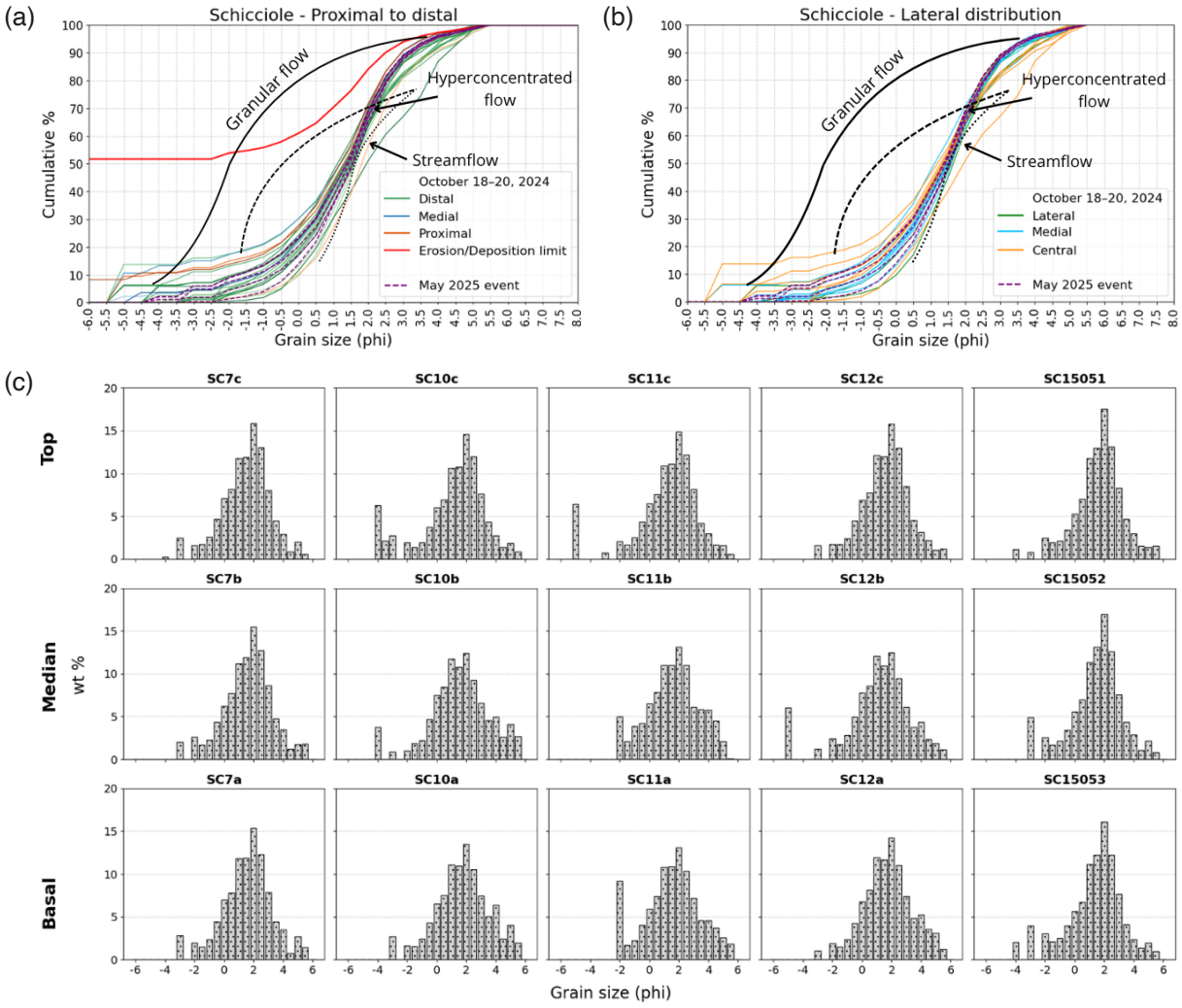

Figure 16. Grain-size analyses on Schicciole Beach samples from both October 2024 and May 2025. (a) Cumulative grain-size curves of the samples along a proximal-distal transect of the 2024 deposit and the May 2025 sample; (b) the Schicciole samples from the central to the lateral portions of the 2024 fan and the May 2025 sample. The reference curves (in black) from Scott et al. (1995) are superimposed to classify the flow type: solid line = granular flows, dashed line = hyperconcentrated flows, dotted line = stream flows. (c) Histograms of the samples used for the vertical characterization of the main fan from the October 2024 events.

Moreover, along the vertical profile of the lahar deposit, the samples from the upper levels are in most cases slightly coarser than the basal ones (Fig. 16c). This finding suggests a variation in the grain-size distributions during the deposition corresponding to an inverse grading. In comparison, the deposits related to the May 2025 event are characterized by overall finer grain-size distributions, comparable to those observed in the distal portions of the October 2024 deposits (Fig. 16a-b).

In Piscità, the cumulative grain-size curves display no systematic trends for both of the October 2024 and May 2025 events, indicating that the deposit does not follow a clear proximal-distal variability (Fig. 17a). This behavior may reflect the initial confinement of the flow within the Montagna Russo channel and its subsequent deviation along Riposto Street. As the flow decelerated near channel bends, coarser and heavier particles tended to settle, resulting in irregular grain-size distributions. Differently from the Schicciole Beach lahar, no significant vertical variations were observed within the sampled deposit.

At the hiking path, the samples collected from the deposit exhibit an inverse trend along the propagation direction compared to the previous sites. The cumulative curves, in fact, are finer grain-sized in the proximal portions and slightly coarser grain-sized in the distal sites (Fig. 17b). Vertically, the upper portions are slightly coarser than the basal ones.

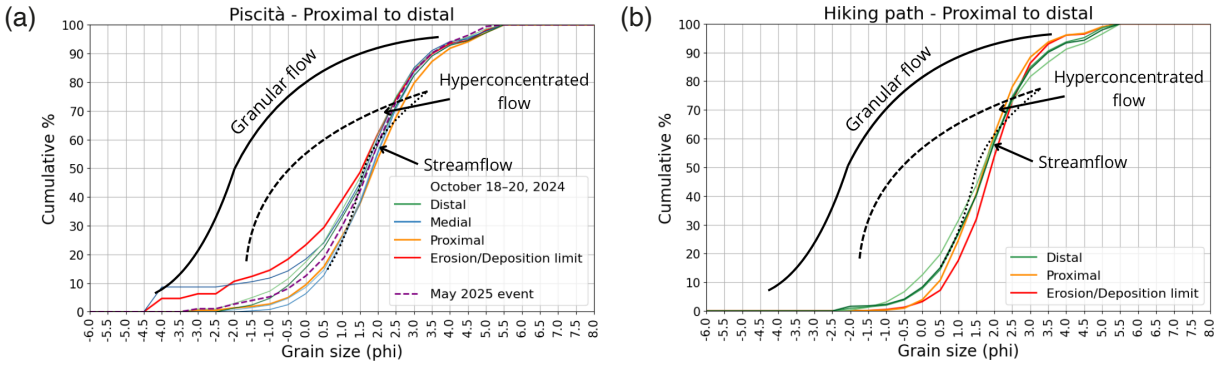

Figure 17. Cumulative grain-size curves of the sampled deposits: (a) 2024 and 2025 Piscità deposits along a proximal-distal transect; (b) Hiking path deposits along a proximal-distal transect. Erosion/Deposition limit stands for samples collected near the boundary. On each diagram, the reference curves (in black) from Scott et al. (1995) are superimposed to classify the flow type: solid line = granular flows, dashed line = hyperconcentrated flows, dotted line = stream flows.

Sorting and the mean grain-size of the samples have been plotted (Fig. 18a), showing that, overall, the median of the studied deposits ranges from 1.1 φ to 1.9 φ. The Schicciole samples have a coarser mean grain-size (up to 1.1 φ) than the Piscità and the hiking path samples (1.5 and 1.7 φ respectively), with the latter characterized by the finest value. Overall, the analyzed deposits exhibit sorting values ranging from 1.0 to 2.5 φ, with the Schicciole Beach lahars showing the most variable and higher values of sorting (from 1.3 to 2.5 φ). According to standard grain-size classifications (Folk and Ward, 1957), these samples would be classified as poorly to very poorly sorted. However, within the category of volcanic granular flows, such values indicate the deposits of the three areas to be relatively well sorted for a volcanic flow context (Cas and Wright, 1988). This is consistent with the predominantly sandy nature of the source material, as also highlighted by the histograms in Fig. 16c. These display near-Gaussian, unimodal distributions, reflecting a homogeneous sediment population associated with hyperconcentrated flow dynamics (Scott et al., 1995; Costa, 1984.). Minor secondary peaks observed in the coarser fractions are related to the presence of heterogeneous clasts as previously mentioned.

The skewness and the kurtosis parameters are also considered (Fig. 18b). At the Schicciole Beach, the analyzed samples (from both October 2024 and May 2025 events) exhibit a wide range of skewness, from nearly symmetrical to negative, indicating a tendency toward an enrichment in coarser particles. In contrast, the Piscità and hiking path samples generally show near-symmetrical grain-size distributions. Regarding the kurtosis, the Schicciole deposit has a high degree of variability, ranging from leptokurtic to platykurtic (i.e., highly variable peakedness in the grain-size curves). Conversely, the Piscità and hiking path samples generally fall within the mesokurtic to platykurtic distributions, reflecting a more uniform and less sharply peaked distribution of volcanic particles.

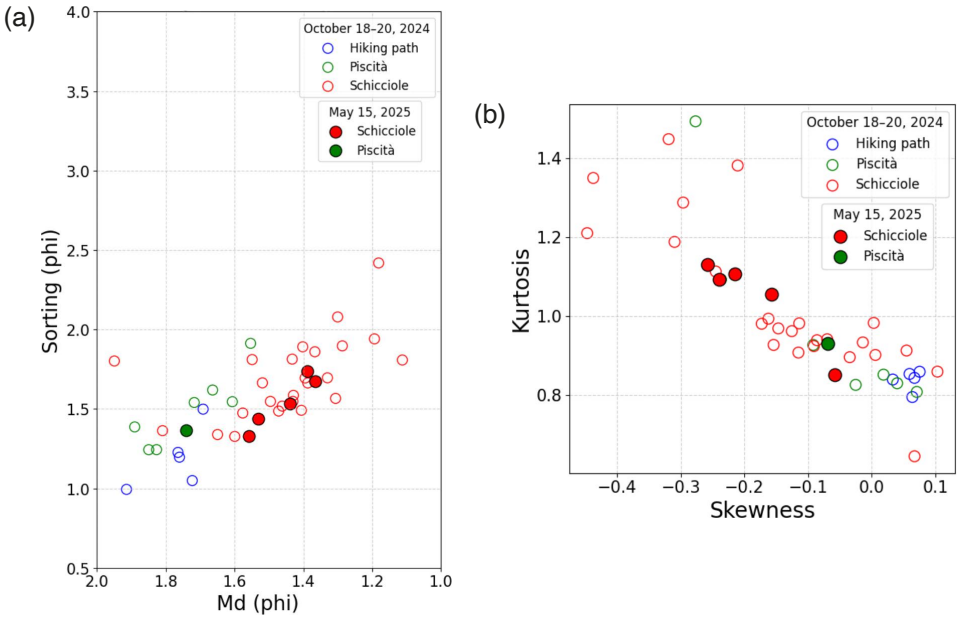

Figure 18. (a) Sorting versus median and (b) skewness versus kurtosis for the analyzed lahar samples. In both diagrams, empty circles refer to the October 2024 events samples while filled ones refer to the May 2025 event samples.

4.3 Comparisons and classifications of the recent lahar deposits

To characterize the recent lahar deposits at Stromboli, our results were benchmarked against datasets and classification schemes available in the literature.

Taking into account the overall grain-size of the deposits from all the locations, the lahars of Stromboli have been classified by using the Udden-Wentworth scale. Most of our samples fall within the sand class (from –1 to 4 φ, i.e. from 2 to 0.0625 mm) (Fig. 19). In particular, this fraction accounts for 90.8 wt% at Schicciole Beach, 89.7 wt% in the Piscità sector and 90.8 wt% along the hiking path.

To further support the field-based interpretation of the deposits as hyperconcentrated-flows, the cumulative curves of the samples are matched against the flow type classification proposed by Scott et al. (1995) (black lines in Fig. 16a-b and Fig. 17). This comparison indicates that the Stromboli lahars, in each of the three selected areas, show trends comparable to streamflow deposits, although they display a transitional behavior toward hyperconcentrated flow conditions. In particular, while the general trend of the curves is similar to that of streamflow, the higher sediment concentration is consistent with hyperconcentrated flows (matching the field observation), which are defined by Scott et al. (1995) as flows containing from 20 to 60 percent of sediment by volume, and by Pierson and Costa (1987) as a flowing mixture of water and sediment that has a measurable yield strength but appears to flow like a liquid. For this reason, these flows can be interpreted as hyperconcentrated flows with a dominant streamflow behavior (i.e. hyperconcentrated streamflow in a descriptive sense). This classification is further validated by plotting our data (sorting versus mean grain-size), showing a good agreement with the classification proposed by Scott et al. (1995) and subsequently refined by Pistolesi et al. (2013) (Fig. 20).

The grain-size parameters obtained in this study are further interpreted by comparing them with previously published datasets of tephra fallout and pyroclastic density current (PDC) deposits at Stromboli volcano (Fig. 21). Such a comparison allows for a better understanding of the potential source material of the 2024 and 2025 lahar deposits. Pistolesi et al. (2011) analyzed the deposits of the March 15, 2007 paroxysmal event, characterized by PDC and ash and lapilli fallout deposits. In detail, for the PDC deposit, the authors identify three main units with different sedimentological characteristics. UNIT 1 is characterized by sorting between 1.9 and 1.6 and a mean grain-size ranging between 0.9 and 2 φ, while UNIT 2 shows higher sorting (σ_φ = 1.3-1.1) and a finer mean grain-size (1.1-3.2 φ). In contrast, UNIT 3, which is lithic-rich, displays very poor sorting ($\sigma_\varphi \approx 3.9$) and a very coarse mean grain-size ($Md_\varphi = -6.8\ \varphi$). Ash and lapilli deposits produced during the eruption are characterized by a mean sorting of 2.8 and a Md_φ of 0.58 φ. Di Roberto et al. (2014) investigated the deposits related to the 1930 and 1944 paroxysms, both characterized by PDCs. For the 1930 event, three main sites were analyzed by the authors: at site

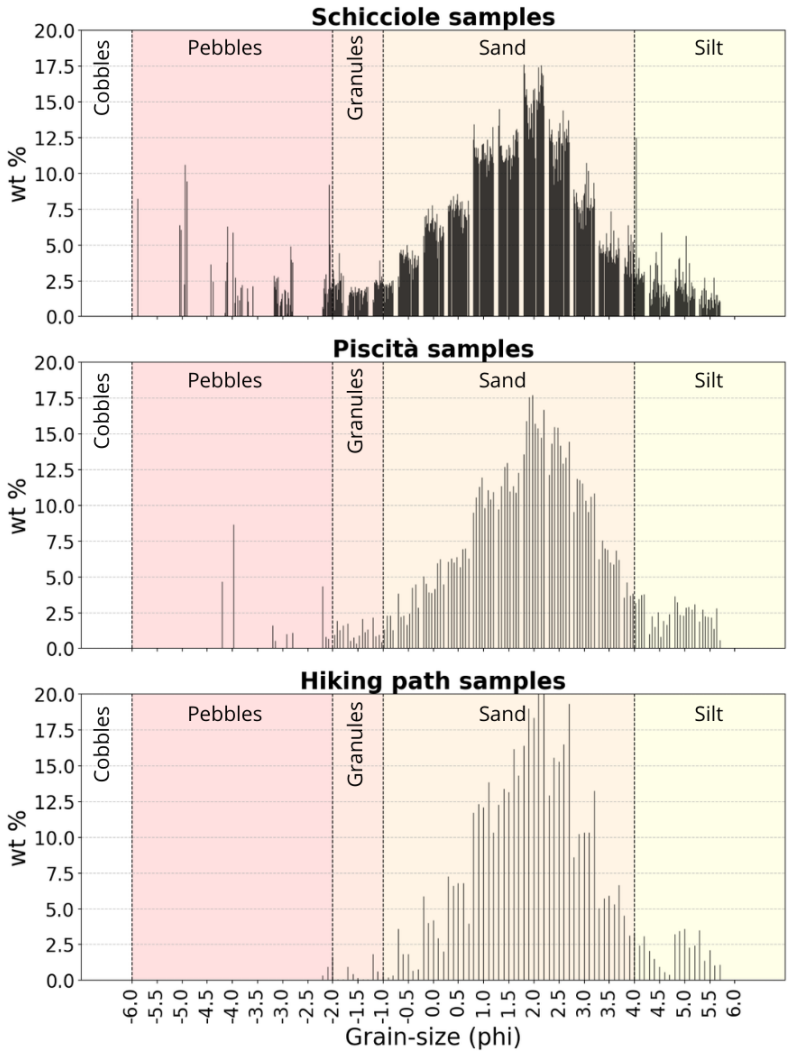

Figure 19. Histograms of all analyzed samples. In each sector the plots were obtained by overlapping the histograms of individual samples, in order to highlight the average trend of grain-size classes. The classes from Udden-Wentworth are shown.

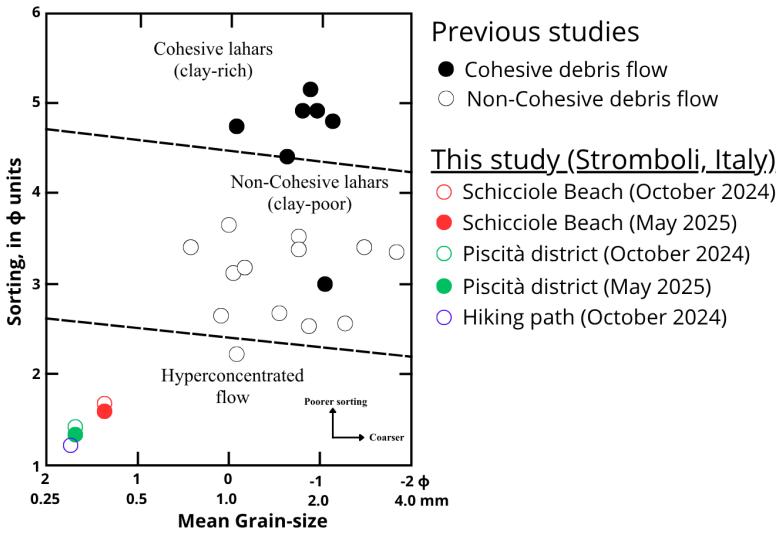

Figure 20. Plot of the sorting versus mean grain-size from Scott et al. (1995) and Pistolesi et al. (2013) used for comparison of our results (modified after Pistolesi et al., 2013).

1 (San Bartolo valley) the deposit consists of a lower unit composed of medium ash ($Md_{\varphi} = 1.63$) with sorting of 1.27 and dispersed lapilli, overlain by an upper unit ($\sigma_{\varphi} = 5.09$; $Md_{\varphi} = -0.79$) consisting of block- to coarse lapilli-sized lithic clasts and juvenile bombs and lapilli, supported by a poorly sorted, massive, coarse ash matrix. At site 2 (located on a topographic high near the NE rim of the Vallonazzo valley), the deposit is composed of poorly sorted ($\sigma_{\varphi} = 3.21$) coarse ash ($Md_{\varphi} = 0.47$). Similarly, at site 3, near Piscità beach, the deposit is characterized by poorly sorted ($\sigma_{\varphi} = 2.87$) coarse ash ($Md_{\varphi} = 0.92$). For the 1944 event, the PDC deposit was identified at Schicciole Beach and mainly consists of juvenile material embedded in a coarse ash matrix ($Md_{\varphi} = 0.68$) with a sorting of 1.97, with minor lithic lapilli and blocks. Samples collected on the ash cloud deposit generated during the gravitational collapse that occurred on May 19, 2021 were analyzed by Re et al. (2022) and are characterized by good sorting ($\sigma_{\varphi} = 0.71$-0.81) and fine mean grain-sizes (3.76-3.92 φ), reflecting deposition from fallout processes.

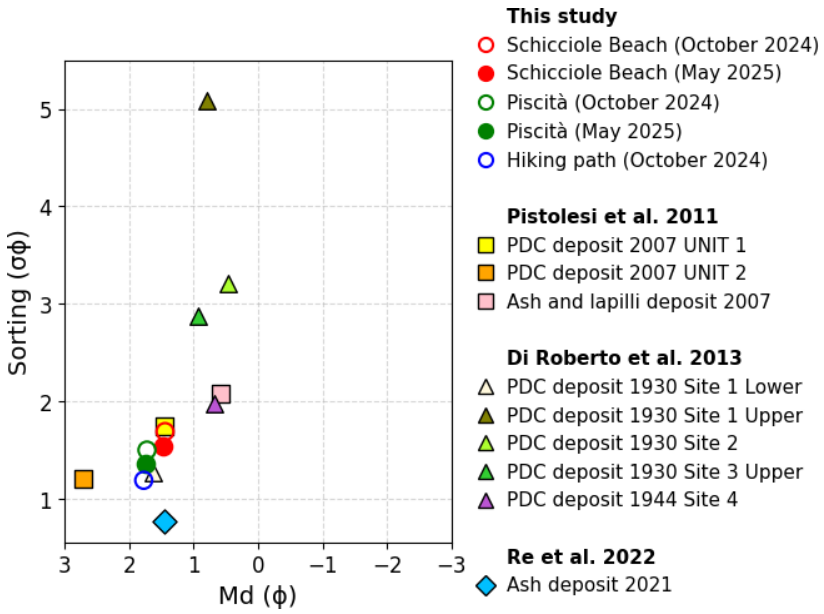

Figure 21. Plot of the sorting versus mean grain-size of the different lahar deposits examined in this study, compared with the values of the pyroclastic deposits that formed in Stromboli in 1930-1944 (Di Roberto et al., 2014), 2007 (Pistolesi et al., 2011) and 2021 (Re et al., 2022).

The lahar deposits analyzed in this study exhibit sedimentological properties intermediate between those of the deposits from 2007 and 1930, with mean grain-size values ranging between 1.1 and 1.9 φ and sorting values between 1.3 and 2.5 φ. These parameters, however, match partially with those of UNIT 1 described by Pistolesi et al. (2011) and lower unit of Site 1 from Di Roberto et al., (2014), suggesting that the 2024 and 2025 lahar deposits are primarily composed of remobilized pyroclastic material originally produced by Strombolian and paroxysmal activity. In contrast, PDC deposits described in more distal settings, display different characteristics, reflecting progressive depositional processes. Conversely, proximal PDC deposits are characterized by grain-size features closer to the studied lahars, which preserve the characteristics of the source material remobilized by rainfall.

Table 3 and Table 4 summarize the main parameters obtained from the analyzed samples across the three investigated sectors. This synthesis provides an overview of the variability of the lahar deposits.

Table 3. Summary of spatial variability and flow types for each investigated area.

Area	Lateral variability	Longitudinal variability	Vertical variability	Flow type
Schicciole Beach (October 2024)	Coarser central, finer lateral	Proxmally coarser, distally finer	Slightly coarser top levels	Hyperconcentrated streamflow
Schicciole Beach (May 2025)	Not applicable	Not applicable	Slightly coarser top levels	Hyperconcentrated streamflow
Piscità	Not applicable	Irregular	No clear variability	Hyperconcentrated streamflow
Hiking path	Not applicable	Finer proximal, coarser distal	Slightly coarser top levels	Hyperconcentrated streamflow

Table 4. Summary of grain-size parameters obtained for each investigated area.

Area	Mean grain-size (Φ)	Sorting	Skewness	Kurtosis
Schicciole Beach (October 2024)	1.1-1.9	Well sorted	Near symmetrical to negative	Leptokurtic to platykurtic
Schicciole Beach (May 2025)	1.4-1.6	Well sorted	Near symmetrical to negative	Leptokurtic to platykurtic
Piscità	1.5-1.9	Well sorted	Near symmetrical	Mesokurtic-platykurtic
Hiking path	1.7-1.9	Well sorted	Near symmetrical	Mesokurtic-platykurtic

5. Conclusions

Lahars on Stromboli represent a widespread volcanic hazard, occurring in different areas of the island and with varying size and scale. The causes of these phenomena are multiple, including extreme rainfall events compared to the past, the impact of the recent fires on vegetation cover and its capacity of soil retention, the increased supply of loose volcanic material on the upper flanks of the volcano due to the recent volcanic activity, the large amount of fine-grained material emplaced after landslide events along the Sciara del Fuoco. The field evidence collected during this study confirms that these flows originate across a wide range of elevations, typically following pre-existing drainage channels. Moreover, in several cases they reach the coastal settlements, therefore posing a direct threat to infrastructure and human activities.

Two dedicated field campaigns were carried out in three sectors of Stromboli Island affected by lahars occurring on October 18-20, 2024 and May 15, 2025: Schicciole Beach, the Montagna Russo channel reaching the Piscità district and a hiking path on the northeastern flank of the volcano. These areas are characterized by distinct geomorphological settings, which strongly influenced the flow dynamics and thus the emplacement and preservation of the lahar deposits. At Schicciole Beach, lahars' source material comes from the Forgia Vecchia area generating fan-shaped deposits during both the October 2024 and May 2025 events, reflecting unconfined flow conditions but rapid deposition at the coastal break in slope. Pleiades optical satellite data allowed the identification of the central fan at Schicciole Beach and the calculation of its extent, resulting in an area of approximately 0.03 km^2. Along the Montagna Russo channel, the flow was confined within the stream banks, promoting efficient downstream transport and a longer runout, with sediment deposition strongly controlled by the channel geometry and local variations in flow energy. The deposits along the hiking path also show evidence of a channelized flow, however, their limited extent and preservation allowed only a partial sedimentological characterization.

The grain-size analyses conducted on deposits of the three representative sectors provide the first quantitative dataset available for lahars on Stromboli. The deposits are characterized by a mode of 2 φ, i.e. most of the particles composing these lahars are 0.25 mm in size. The Schicciole Beach deposits are the coarsest, particularly in the central and proximal portion of the largest fan, where the presence of decimetric clasts is typical of high-energy flow conditions. The Piscità deposits, in contrast, display no clear grain-size pattern, according to the flow confinement and deceleration along channel bends along the Montagna Russo stream. The hiking path deposits are generally finer, with slightly coarser upper layers. The May 2025 deposits provide evidence that new lahars can form adjacent to previous deposits, but also actively incise and thus erode the upper surface of existing, older lahar material.

From a sedimentological point of view, Stromboli lahars are well sorted and are characterized by mean grain-size values ranging from 1.1 to 1.9 φ, near-symmetrical to negative skewness and kurtosis values from leptokurtic to platykurtic. The overall well sorting reflects the characteristics of the source material, which is predominantly sandy. This is clearly supported by the grain-size distributions, which display Gaussian distribution with a single dominant mode, indicating a well-defined and homogeneous sediment population. The coarser mean grain-size and wider range in sorting, skewness and kurtosis observed at Schicciole Beach indicate more energetic flow conditions and a stronger influence of the source material remobilized from the upper slopes, with limited modification during transport. Conversely, the finer and more uniform grain-size distributions characterizing the Piscità and hiking path deposits can be correlated to a relatively greater confinement of the flow and more localized depositional processes, controlled by channel geometry.

The 2024 and 2025 lahar deposits are mainly composed of sand ($-1 - 4\ \varphi$), which accounts for 89.7 wt% to 90.8 wt% of the samples across the three representative deposits. The comparison of these values with reference datasets and literature classifications aligns these deposits with hyperconcentrated stream flows. The comparison between the grain-size characteristics of the studied lahar deposits and previously published datasets from Stromboli indicates that the source material was predominantly derived from Strombolian and paroxysmal eruptive activity.

The results obtained in this study provide a fundamental baseline for understanding the lahars on Stromboli serving as a basis for parametrizing future numerical simulations, which are essential for improving hazard assessment for lahar prone sectors of Stromboli island.

Acknowledgements. This study was funded by the INGV project 'Reti Multiparametriche'. This study was partially supported by the Space It Up project, funded by the ASI and the MUR – Contract n. 2024-5-E.0 - CUP n. I53D24000060005, and by the Istituto Nazionale di Geofisica e Vulcanologia (INGV) through the Departmental Strategic Project UNO (UNderstanding the Ordinary to forecast the extraordinary: An integrated approach for studying and interpreting the explosive activity at Stromboli volcano (CUP D59C19000140005). We acknowledge Dr. Alessandro La Spina and Dr. Antonio Cristaldi (INGV-OE) for supporting during the June 2025 survey on the Schicciole Beach. We would like to thank Dr. Luigi Guerriero and Dr. Lucia Capra for their careful reviewing of the manuscript and for their constructive and insightful comments. We also acknowledge S. Conway for carefully revising the English text.

References

Andronico, D., E. Del Bello, C. D'Oriano, P. Landi et al. (2021). Uncovering the eruptive patterns of the 2019 double paroxysm eruption crisis of Stromboli volcano, Nat. Commun., 12, 1, 4213, doi:10.1038/s41467-021-24420-1.

Barberi, F., M. Rosi and A. Sodi (1993). Volcanic hazard assessment at Stromboli based on review of historical data, Acta Vulcanol., 3, 173-187.

Bertagnini, A., A. Di Roberto and M. Pompilio (2011). Paroxysmal activity at Stromboli: lessons from the past, Bull. Volcanol., 73, 1229-1243, doi:10.1007/s00445-011-0470-3.

Bisson, M., R. Gianardi, R. Civico, P. Madonia et al. (2025). Lidar-derived digital surface model of Stromboli island updated to August 2023, Sci. Data, 12, 522, doi:10.1038/s41597-025-04856-6.

Bosman, A., F. L. Chiocci and C. Romagnoli (2009). Morpho-structural setting of Stromboli volcano revealed by high-resolution bathymetry and backscatter data of its submarine portions, Bull. Volcanol., 71, 1007-1019, doi:10.1007/s00445-009-0279-5.

Capra, L., L. Borselli, N. Varley, J. C. Gavilanes-Ruiz et al. (2010). Rainfall-triggered lahars at Volcán de Colima, Mexico: surface hydro-repellency as initiation process, J. Volcanol. Geotherm. Res., 189, 105-117, doi:10.1016/j.jvolgeores.2009.10.014.

Cas, R. A. and J. V. Wright (1988). Volcanic successions: modern and ancient: a geological approach to processes, products and successions, Springer, Dordrecht, doi:10.1007/978-94-009-3167-1.

Costa, J. E. (1984). Physical geomorphology of debris flows, Developments and applications of geomorphology, Springer, Berlin, Heidelberg, 268-317, doi:10.1007/978-3-642-69759-3_9.

Di Roberto, A., A. Bertagnini, M. Pompilio and M. Bisson (2014). Pyroclastic density currents at Stromboli volcano (Aeolian Islands, Italy): a case study of the 1930 eruption, Bull. Volcanol., 76, 827, doi:10.1007/s00445-014-0827-5.

Folk, R. L. and W. C. Ward (1957). Brazos River bar [Texas]: a study in the significance of grain size parameters, J. Sediment. Res., 27, 3-26, doi:10.1306/74D70646-2B21-11D7-8648000102C1865D.

Ferrentino, E., M. Polcari, G. Esposito and C. Bignami (2025). A dual polarimetric method for detecting burnt areas: the May 2022 Stromboli Island (Italy) wildfire, Remote Sens. Lett., 16, 947-957, doi:10.1080/2150704X.2025.2522931.

Giordano, G. and G. De Astis (2021). The summer 2019 basaltic Vulcanian eruptions (paroxysms) of Stromboli, Bull. Volcanol., 83, 1, doi:10.1007/s00445-020-01423-2.

Guardo, R., G. Bilotta, G. Ganci, F. Zuccarello et al. (2024). Modeling fire hazards induced by volcanic eruptions: the case of Stromboli (Italy), Fire, 7, 70, doi:10.3390/fire7030070.

Guarino, R., D. Cerra, R. Zaia, A. Chiarucci et al. (2024). Remote sensing reveals fire-driven enhancement of a C4 invasive alien grass on a small Mediterranean volcanic island, Biogeosciences, 21, 2717-2730, doi:10.5194/bg-21-2717-2024.

Iacono, F., M. Bisson, C. Spinetti and T. Kwasnitschka (2025). Wildfires induced by volcanic activity at Stromboli Island during the 2019 summer through satellite and drone data, Remote Sens. Earth Syst. Sci., 8, 2, 733-752, doi:10.1007/s41976-025-00215-6.

Lavigne, F., J. C. Thouret, B. Voight, H. Suwa et al. (2000). Lahars at Merapi volcano, Central Java: an overview, J. Volcanol. Geotherm. Res., 100, 1-4, 423-456, doi:10.1016/S0377-0273(00)00150-5.

Manville, V., J. J. Major and S. A. Fagents (2013). Modeling lahar behavior and hazards, in Modeling volcanic processes: the physics and mathematics of volcanism, S. A. Fagents, T. K. P. Gregg and R. M. C. Lopes (Editors), Cambridge University Press, Cambridge, 300-330, doi:10.1017/CBO9781139021562.014.

Marsella, M., P. Baldi, M. Coltelli and M. Fabris (2012). The morphological evolution of the Sciara del Fuoco since 1868: reconstructing the effusive activity at Stromboli volcano, Bull. Volcanol., 74, 1, 231-248, doi:10.1007/s00445-011-0516-6.

Palaseanu-Lovejoy, M., M. Bisson, C. Spinetti, M. F. Buongiorno et al. (2019). High-resolution and accurate topography reconstruction of Mount Etna from Pleiades satellite data, Remote Sens., 11, 24, 2983, doi:10.3390/rs11242983.

Pasquarè, G., L. Francalanci, V. H. Garduno and A. Tibaldi (1993). Structure and geologic evolution of the Stromboli volcano, Aeolian Islands, Italy, Acta Vulcanol., 3, 79-89.

Pierson, T. C. and J. E. Costa (1987). A rheologic classification of subaerial sediment-water flows, Rev. Eng. Geol., 7, 1-12, doi:10.1130/REG7-p1.

Pierson, T. C., R. J. Janda, J. C. Thouret and C. A. Borrero (1990). Perturbation and melting of snow and ice by the 13 November 1985 eruption of Nevado del Ruiz, Colombia, and consequent mobilization, flow and deposition of lahars, J. Volcanol. Geotherm. Res., 41, 1-4, 17-66, doi:10.1016/0377-0273(90)90082-Q.

Pistolesi, M., D. Delle Donne, L. Pioli, M. Rosi et al. (2011). The 15 March 2007 explosive crisis at Stromboli volcano, Italy: assessing physical parameters through a multidisciplinary approach, J. Geophys. Res. Solid Earth, 116, B12, doi:10.1029/2011JB008527.

Pistolesi, M., R. Cioni, M. Rosi, K. V. Cashman et al. (2013). Evidence for lahar-triggering mechanisms in complex stratigraphic sequences: the post-twelfth century eruptive activity of Cotopaxi Volcano, Ecuador, Bull. Volcanol., 75, 698, doi:10.1007/s00445-013-0698-1.

Re, G., M. Pompilio, P. Del Carlo and A. Di Roberto (2022). Physical and morphological characterization of the 19 May 2021 ash cloud deposit at Stromboli (Italy), Sci. Rep., 12, 1, 10777, doi:10.1038/s41598-022-14908-1.

Rosi, M., A. Bertagnini and P. Landi (2000). Onset of the persistent activity at Stromboli volcano (Italy), Bull. Volcanol., 62, 4, 294-300, doi:10.1007/s004450000098.

Rosi, M., M. Pistolesi, A. Bertagnini, P. Landi et al. (2013). Stromboli volcano, Aeolian Islands (Italy): present eruptive activity and hazards, in Geol. Soc. Lond. Mem., 37, 473-490, doi:10.1144/M37.14.

Scott, K. M., J. W. Vallance and P. T. Pringle (1995). Sedimentology, behavior, and hazards of debris flows at Mount Rainier, Washington, U.S. Geol. Surv. Prof. Pap., 1547, doi:10.3133/pp1547.

Spinetti, C., F. Mazzarini, R. Casacchia, L. Colini et al. (2009). Spectral properties of volcanic materials from hyperspectral field and satellite data compared with LiDAR data at Mt. Etna, Int. J. Appl. Earth Obs. Geoinf., 11, 2, 142-155, doi:10.1016/j.jag.2009.01.001.

Tibaldi, A. (2001). Multiple sector collapses at Stromboli volcano, Italy: how they work, Bull. Volcanol., 63, 112-125, doi:10.1007/s004450100129.

Udden, J. A. (1914). Mechanical composition of clastic sediments, Bull. Geol. Soc. Am., 25, 1, 655-744, doi:10.1130/GSAB-25-655.

Vallance, J. W. (2024). Lahars: origins, behavior and hazards, in Advances in debris-flow science and practice, M. Jakob, S. McDougall and P. Santi (Editors), Springer, Cham, doi:10.1007/978-3-031-48691-3_12.

Vallance, J. W. and R. M. Iverson (2015). Lahars and their deposits, in The encyclopedia of volcanoes, Academic Press, San Diego, 649-664, doi:10.1016/B978-0-12-385938-9.00037-7.

Wentworth, C. K. (1922). A scale of grade and class terms for clastic sediments, J. Geol., 30, 5, 377-392, doi:10.1086/622910.

Witham, C. S. (2005). Volcanic disasters and incidents: a new database, J. Volcanol. Geotherm. Res., 148, 3-4, 191-233, doi:10.1016/j.jvolgeores.2005.04.017.

***CORRESPONDING AUTHOR: Roberto GIANARDI**,
University of Pisa, Earth Sciences Department, Pisa, Italy
Istituto Nazionale di Geofisica e Vulcanologia, Sezione di Pisa, Pisa, Italy
e-mail: roberto.gianardi@ingv.it